Mitochondrial ATP-dependent K^+ channels downregulate ionotropic glutamate receptors during hypoxia in retinal horizontal cells of goldfish

By Mohamed Ramadan

Thesis submitted to the University of Ottawa

in partial fulfillment of the requirements for the Master of Science degree in Biology

Ottawa-Carleton Institute of Biology

Department of Biology

Faculty of Science

University of Ottawa

ACKNOWLEDGEMENTS

First and foremost, I would like to express my deepest gratitude to Dr. Michael Jonz for his guidance and encouragement throughout my thesis. Patch clamp often tested my patience, yet his steady support, reassurance, and depth of knowledge guided me through every challenge. Beyond his mentorship, he is truly inspiring both as a scientist and as a person. I am especially grateful for the great music he shared along the way, which showed me that science, like music, is built on both practice and creativity.

To my lab mates, Maddy, Anthea, Willa and Louise, thank you for making long days in the lab lighter and more enjoyable. Your support made this journey far less lonely, and I am thankful for the laughs and conversations we shared. To the honours student, thank you for bringing energy and fresh perspectives into the lab. I would also like to thank Niki for giving me great advice that helped me navigate through the challenges of a master's degree.

Finally, I owe the biggest thanks to my friends and family for their endless love and encouragement. Thank you for always asking me about my fish (whether you wanted to hear about them or not) and for supporting me in every way possible. And of course, I must also thank coffee and blueberry muffins, faithful companions that got me through many long days and early mornings.

As Niels Bohr once said, "*An expert is a person who has made all the mistakes that can be made in a very narrow field."* While I am far from an expert, I can say that every mistake along the way has been an important part of this learning process, each one making me better than before.

ABSTRACT

Retinal neurons rely on a continuous supply of oxygen to maintain function, yet some species like goldfish can withstand prolonged hypoxic periods due to adaptations that remain unclear. Horizontal cells (HCs) are interneurons in the retina that shape visual signalling by feeding back to photoreceptors. In the present study, we investigated whether ionotropic glutamate receptors (iGluRs) in goldfish HCs are suppressed during hypoxia and whether this process is mediated by mitochondrial ATP-sensitive K^+ (mK_{ATP}) channel activation. Through perforated patch-clamp electrophysiology, we determined that glutamate application under hypoxia reduced median peak current density by ~10.5% ($P = 0.0059$), whereas control recordings in normoxia showed stable responses. When mK_{ATP} channels were blocked with 100 μM glibenclamide during hypoxia, the suppressed response was abolished. Inhibiting mitochondrial calcium (Ca^{2+}) uptake via the mitochondrial Ca^{2+} uniporter (MCU) with ruthenium red and blocking Ca^{2+} release through ryanodine receptors in the endoplasmic reticulum also abolished the hypoxia-induced suppression. Taken together, these results indicate that mK_{ATP} activation triggers a controlled Ca^{2+} signal that downregulates iGluR activity in the membrane. Through the reduction of receptor activity, HCs may lower their metabolic demand, allowing them to maintain cell function during hypoxia. The proposed mechanism can ultimately provide insight into treating retinal conditions associated with hypoxia such as retinal ischemia and stroke.

RÉSUMÉ

Les neurones rétiniens ont besoin d'un apport continu en oxygène pour fonctionner, mais certaines espèces, comme les poissons rouges, peuvent supporter des périodes d'hypoxie prolongées grâce à des adaptations qui restent encore floues. Les cellules horizontales (HC) sont des interneurones de la rétine qui modulent les signaux visuels en renvoyant des informations aux photorécepteurs. Dans la présente étude, nous avons cherché à déterminer si les récepteurs ionotropiques du glutamate (iGluR) des HC du poisson rouge sont inhibés pendant l'hypoxie et si ce processus est médié par l'activation des canaux K+ sensibles à l'ATP mitochondriaux (mKATP). Grâce à l'électrophysiologie par patch-clamp perforé, nous avons déterminé que l'application de glutamate en hypoxie réduisait la densité de courant maximale médiane d'environ 10,5 % (P = 0,0059), tandis que les enregistrements témoins en normoxie montraient des réponses stables. Lorsque les canaux mKATP étaient bloqués avec 100 µM de glibenclamide pendant l'hypoxie, la réponse supprimée était abolie. L'inhibition de l'absorption du calcium (Ca2+) mitochondrial via le transporteur uniportateur de Ca2+ mitochondrial (MCU) avec du rouge de ruthénium et le blocage de la libération de Ca2+ par les récepteurs de la ryanodine dans le réticulum endoplasmique ont également supprimé la suppression induite par l'hypoxie. Dans l'ensemble, ces résultats indiquent que l'activation du mKATP déclenche un signal Ca2+ contrôlé qui régule à la baisse l'activité de l'iGluR dans la membrane. Grâce à la réduction de l'activité des récepteurs, les HC peuvent diminuer leur demande métabolique, ce qui leur permet de maintenir leur fonction cellulaire pendant l'hypoxie. Le mécanisme proposé peut finalement fournir des informations utiles pour le traitement des affections rétiniennes associées à l'hypoxie.

TABLE OF CONTENTS

LIST OF FIGURES & TABLES

LIST OF ABBREVIATIONS

AMPAR	α-amino-3-hydroxy-5-methyl-4-isoxazolepropionic acid receptor
ATP	Adenosine triphosphate
Ca^{2+}	Calcium
CICR	Ca^{2+}-induced Ca^{2+} release
$[Ca^{2+}]_i$	Intracellular concentration of calcium ions
°C	Degrees Celsius
CNS	Central nervous system
DMSO	Dimethyl sulfoxide
ECS	Extracellular solution
ER	Endoplasmic reticulum
GABA	γ-aminobutyric acid
$[GABA]_e$	Extracellular GABA concentration
GC	Ganglion cell
Glu	Glutamate
h	Hours
HC	Horizontal cell
Hox	Hypoxia
ICS	Intracellular solution
iGluR	Ionotropic glutamate receptor
K^+	Potassium
L-15	Leibovitz's medium
MCU	Mitochondrial Ca^{2+} uniporter
mK_{ATP}	Mitochondrial adenosine triphosphate-dependent potassium channel
mM	Millimolar
min	minutes

mmHg	Millimeters of mercury
Na^+	Sodium
nM	Nanomolar
NMDAR	*N*-methyl-D-aspartate receptor
N_2	Nitrogen
Nox	Normoxia
pH	Potential of hydrogen
PMCA	Plasma membrane Ca^{2+}-ATPase
Ryr	Ryanodine
RR	Ruthenium red
RyR	Ryanodine receptors
P_{O2}	Partial pressure of oxygen
SERCA	Sarcoplasmic/endoplasmic reticulum Ca^{2+} ATPase
s	Second
TMRE	Tetramethylrhodamine ethyl ester
U	Units
VGCC	Voltage-gated Ca2+ channel
v/v	Volume per volume
µM	Micromolar
µm	Micron
5-HD	5-hydroxydecanoate

1. LITERATURE REVIEW

1.1 General Introduction

Oxygen is essential for sustaining neuronal function. An insufficient supply of oxygen (hypoxia) disrupts ion homeostasis and adenosine triphosphate (ATP) production. In most vertebrates, hypoxia causes uncontrolled glutamate release, excessive cytosolic Ca^{2+} accumulation and leads to cell death in extreme cases. The retina is particularly sensitive to oxygen levels due to its high metabolic demand and constant activity. Remarkably, certain vertebrates have evolved adaptations that enable them to survive in low oxygen conditions. Notably, the painted turtle (*Chrysemys picta),* crucian carp (*Carassius carassius*), and common goldfish (*Carassius auratus*) can survive prolonged periods of hypoxia or even complete anoxia by reducing neural activity to conserve ATP expenditure (Johansson et al., 1997; Pamenter et al., 2008; Wilkie et al., 2008; Country & Jonz, 2021). One common mechanism of this tolerance is the activation of mitochondrial ATP-sensitive K^+ (mK_{ATP}) channels which have been shown to function as metabolic sensors and initiators of protective signalling pathways. Understanding the exact mechanisms that underlie hypoxia tolerance may provide valuable insight into therapeutic strategies in treatments for conditions such as stroke, ischemia, and other hypoxia related conditions.

This thesis investigates how ionotropic glutamate receptors (iGluR) in goldfish horizontal cells (HCs) are regulated during hypoxia. The presented introduction will provide background on HCs and the vertebrate retina as well as excitotoxicity and hypoxia tolerance in other vertebrates. The introduction concludes by outlining the research objectives of this thesis.

1.2 The Excitotoxic Response

Neurons are among the most metabolically demanding cells in the body, relying on a continuous source of energy in the form of ATP to fuel essential membrane ATPases that maintain electrochemical gradients. Within the central nervous system (CNS), the retina is particularly energy sensitive (Wong-Riley, 2010). ATP is primarily used to fuel pumps such as the Na^+/K^+-ATPase and Ca^{2+}-ATPase, which are responsible for maintaining electrochemical gradients and regulating intracellular Ca^{2+} concentrations ($[Ca^{2+}]_i$) (Country & Jonz, 2017). Inadequate oxygen availability, or hypoxia, can have a detrimental effect on neural function as most vertebrates rely on oxygen to generate ATP. When ATP levels fall, ionic gradients are disrupted, leading to uncontrolled membrane depolarization, excessive glutamate release, and diminished reuptake of neurotransmitters (Szydlowska & Tymianski, 2010). Glutamate activates iGluRs on postsynaptic neurons, which depolarizes their membrane and increases Ca^{2+} influx. These receptors include α-amino-3-hydroxy-5-methyl-4-isoxazolepropionic acid receptors (AMPAR), N-methyl-D-aspartate receptors (NMDAR), and kainite receptors, all of which play a role in excitatory signalling within the retina. The depolarization produced by iGluR activation opens voltage-gated Ca^{2+} channels (VGCC), increasing Ca^{2+} influx and further depolarizing the cell (Linn & Christensen, 1992; Tachibana, 1983).

During hypoxia, excessive amounts of glutamate are released, and neurotransmitter uptake becomes impaired, resulting in the prolonged and uncontrolled activation of these receptors. This overstimulates neurons, driving hyperexcitability and causing intracellular Ca^{2+} to accumulate to harmful levels. When intracellular Ca^{2+} concentration ($[Ca^{2+}]_i$) reaches toxic levels, this can trigger a cascade pathway leading to cell death through apoptosis. High levels of $[Ca^{2+}]_i$ activates degradative enzymes such as lipases, proteases and endonucleases which

breakdown cellular membranes and cytoskeletal structures (Orrenius & Nicotera, 1994). Additionally, excessive $[Ca^{2+}]_i$ also disrupts the mitochondrion leading to the production of reactive oxygen species (ROS) and the release of pro-apoptotic proteins, ultimately resulting in cell death (Orrenius et al., 2003; Verkhratsky, 2007; Choi, 1992). This is known as the excitotoxic response.

1.3 Hypoxia Tolerance

The retina is an extension of the CNS and relies on a continuous oxygen supply due to its constant signalling activity, even in darkness (Wong-Riley, 2010; Hoon et al., 2014; Dowling & Ripps, 1973). Retinas of species such as the crucian carp and common goldfish have been used as well-established models for hypoxia tolerance (Country & Jonz, 2022). Goldfish can survive days at 4°C (Walker & Johansen, 1977) and crucian carp can survive in low oxygen water for months at the same temperature (Nilsson & Lutz, 2004), in part due to their ability to supress neural activity to reduce ATP consumption (Country & Jonz, 2021; Johansson et al., 1997; Johansson et al., 1995). Electroretinogram (ERG) recordings from crucian carp show that responses to light flashes in the retina are supressed by 69% in the retina and 75% in the optic tectum after 38 min of anoxia, and by 90% after 1 hour, with full recovery upon reoxygenation. This suppression is thought to be an adaptive mechanism that shuts down visual processing to conserve energy during anoxic stress (Johansson et al., 1997). In a separate study, hypoxia decreased excitatory activity in cone-driven HCs to 76% of control levels and in rod-driven HCs to 55% within 10 min of exposure (Wei & Yang, 1997).

Recent work in goldfish has begun to explore the intracellular pathways responsible for hypoxia tolerance in the retina. HCs isolated from goldfish retina have been shown to maintain a low $[Ca^{2+}]_i$ in the absence of extracellular glutamate during 1 hour of hypoxia through the activation of mK_{ATP} (Country & Jonz, 2021). Paradoxically, hypoxia in the presence of glutamate leads to a modest yet significant rise in $[Ca^{2+}]_i$ in goldfish HCs, which was also mediated by the activation of mK_{ATP} channels. This Ca^{2+} rise did not come from extracellular sources, such as L-type VGCC, but rather was abolished by inhibiting ryanodine receptors in the endoplasmic reticulum (ER) and the mitochondrial Ca^{2+} uniporter (MCU) in the mitochondria, suggesting that it comes from internal stores (Nagy-Watson & Jonz, 2025). Taken together, these findings support the potential role of mK_{ATP} channels in initiating a regulated Ca^{2+} signalling pathway, while simultaneously preventing $[Ca^{2+}]_i$ from reaching excitotoxic levels during hypoxia.

The functional significance of this hypoxia-induced rise in Ca^{2+} remains unclear. However, two primary hypotheses have been proposed. One possibility is that the increase in $[Ca^{2+}]_i$ induces the release of the inhibitory neurotransmitter γ-aminobutyric acid (GABA) from HCs during hypoxia. Indeed, GABAergic suppression is a common neuroprotective strategy during hypoxia in many tolerant animals. In both turtle and crucian carp brain, prolonged anoxic exposure leads to increased GABA release, which supresses neural firing and reduces metabolic activity (Nilsson & Lutz, 1991; Nilsson, 1992). Blocking GABA receptors ($GABA_A$ and $GABA_B$) in the turtle brain under anoxia failed to prevent excitotoxity (Pamenter et al., 2011; reviewed in Buck & Pamenter, 2018). Evidence for a rise in GABA release from goldfish HCs during hypoxia has never been provided.

The second hypothesis is that the Ca^{2+} signal may induce ion channel arrest, similar to a mechanism described in the turtle cortex (Pamenter et al., 2008). In this model, the controlled

rise in Ca^{2+} activates a calmodulin signalling pathway that ultimately downregulates NMDAR in the membrane (Pamenter et al., 2008; Shin et al., 2005). This adaptive suppression of receptor activity reduces excitotoxic stress while enabling receptor activity to be restored once oxygen becomes available.

These two proposed mechanisms suggest that the hypoxia-induced rise in $[Ca^{2+}]_i$ in goldfish HCs may provide inhibitory feedback to reduce overall activity in the retina or directly supress excitatory receptor function through channel arrest. While both remain plausible, the data presented in this thesis support the latter: that mK_{ATP}-dependent Ca^{2+} signalling mediates ion channel arrest in goldfish HCs during hypoxia.

1.4 Mitochondrial ATP-sensitive K^+ (mK_{ATP}) Channels

mK_{ATP} channels are weak inward rectifiers located on the inner mitochondrial membrane (Pamenter, 2011). During hypoxia, these channels are thought to function as metabolic sensors that open in response to reduced ATP levels during stress (Tinker et al., 2013). The relevance of mK_{ATP} activation to low oxygen sensing and neuroprotection has been demonstrated in multiple animal models. In mice, activation of mK_{ATP} channels reduced neural apoptosis and improved astrocyte survival during hypoxia (Liu et al., 2002). In embryonic chick telencephalon cells, activation of these channels preserved cell viability during chemically induced hypoxia (Wind et al., 1997), and in cultured rat cortical neurons exposed to glutamate-induced excitotoxicity, activation of mK_{ATP} also prevented excitotoxicity (Kis et al., 2004). In the turtle cortex, hypoxia activates mK_{ATP} channels which increases K^+ conductance. This is driven through K^+/H^+ exchange across the mitochondrial membrane resulting in mild uncoupling of the mitochondrial

membrane potential (Δψm). The reduction in Δψm reduces Ca^{2+} uptake through the MCU, resulting in a modest increase in cytosolic Ca^{2+} (Pamenter et al., 2008; Pamenter, 2011; reviewed in Buck & Pamenter, 2018). This Ca^{2+} signal activates calmodulin and phosphatase-dependent pathways that downregulate NMDAR activity at the plasma membrane (Shin et al., 2005). Through the suppression of excitatory receptor activity, neurons reduce metabolic demand and avoid excitotoxicity. Taken together, these findings demonstrate that mK_{ATP} channels are not only involved in hypoxia sensing but also act as initiators of neuroprotective signalling pathways.

1.5 The Retina

The vertebrate retina is a transparent tissue that lines the inner surface of the posterior eye and consists of three nuclear layers and two plexiform layers (Fig. 1). Nuclear layers contain the cell bodies of the different neural classes, whereas plexiform layers contain the synaptic connections between these neurons. The outer nuclear layer (ONL) contains the cell bodies of photoreceptors which can be divided into two subcategories (rods and cones). Photoreceptors are primary neurons that detect light energy (photons) and convert it into a neural signal. The inner nuclear layer houses the cell bodies of HCs, bipolar cells, and amacrine cells. Bipolar cells receive input from photoreceptors and transmit them to ganglion cells, whereas HCs and amacrine cells modulate neural signals and connect to all neurons (Kolb et. al., 1995). The ganglion cell layer (GCL) is the third nuclear layer and contains the cell bodies of ganglion cells, which receive input from bipolar cells, and converge together to form the optic nerve, where the signal ultimately gets sent to the brain. In the outer plexiform layer (OPL), there are connections between photoreceptors, bipolar cells, and HCs, whereas the inner plexiform layer (IPL) houses

the connections between bipolar cells and ganglion cells as well as connections between bipolar cells and amacrine cells (Kolb et al., 1995; Quinn et al., 2019, Grigoryan, 2022).

Visual processing begins when photons enter the eye and are captured and transduced into electrochemical signals by photoreceptors. Photoreceptors are tonically depolarized in darkness and continuously release glutamate onto postsynaptic HCs and bipolar cells. Thus, when photons interact with photoreceptors, less glutamate is released (Hoon et al., 2014; Dowling & Ripps, 1973; Miller & Schwartz, 1983). Glutamate acts as an excitatory or an inhibitory neurotransmitter, depending on the type of bipolar cell upon which it binds, inducing depolarization or hyperpolarization, respectively. HCs are interneurons and modulate the signal from photoreceptors to bipolar cells, whereas amacrine cells modulate the signal between bipolar cells and ganglion cells. The signal is then conveyed to ganglion cells where it is propagated and integrated along their axons, forming the optic nerve, ultimately reaching the thalamus and visual cortex in the brain for further processing (Kolb, 1995; Quinn et al., 2019; Neves & Lagnado, 1999).

The retina has long been described as an "approachable part of the brain" (Dowling, 1987), based on its developmental origin, and can be easily studied to understand its structure and function. Its organization and neural connections make it an ideal model for studying synaptic transmission and visual processing. The combination of accessibility, well-defined structure, and function has established the retina as a valuable system for studying neuronal responses to stressors like hypoxia, making it an ideal model for understanding neuroprotective mechanisms and neural resilience.

Figure 1. Diagram of the vertebrate retina showing neural layers and synaptic connections. Light enters the eye and travels from inner retina towards the outer retina, passing through the ganglion cell layer (GCL) and inner nuclear layer (INL) before reaching the outer nuclear layer (ONL). In the presence of light, rod and cone photoreceptors become hyperpolarized. When they absorb photons, they convert light energy into electrochemical signals through phototransduction which reduces glutamate release at their synaptic terminals. These changes in glutamate are detected by bipolar cells, which carry the signal forward, and by HCs, which provide inhibitory feedback to photoreceptors through lateral inhibition. The signal then continues from bipolar cells to ganglion cells at the inner plexiform layer (IPL), where amacrine cells further fine tune the response. Finally, this signal is carried along the axons of ganglion cells, which converge together to form the optic nerve and transmit visual information to the brain. For further details, see text. Created using BioRender.com

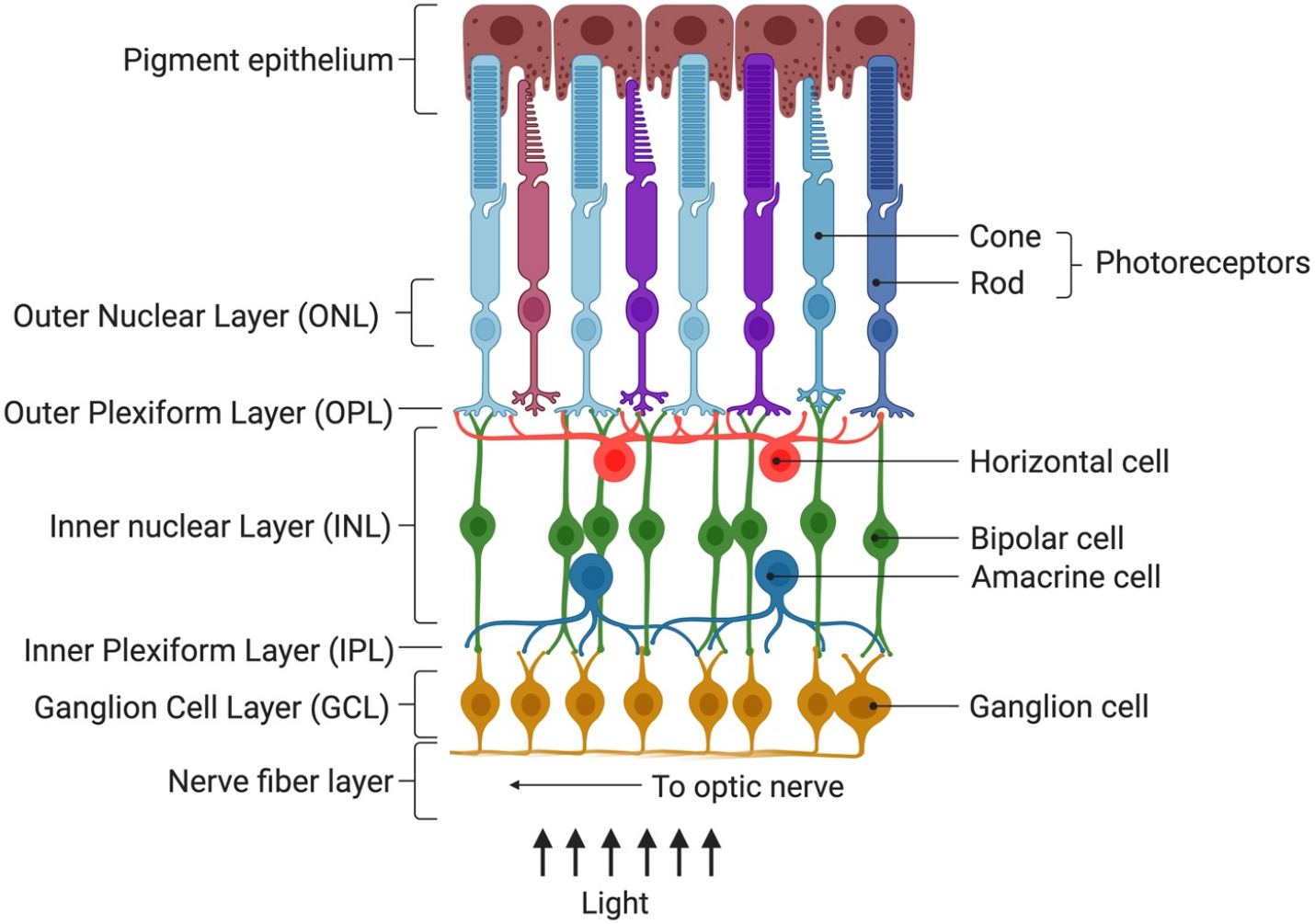
Pigment epithelium
Outer Nuclear Layer (ONL)
Outer Plexiform Layer (OPL)
Inner nuclear Layer (INL)
Inner Plexiform Layer (IPL)
Ganglion Cell Layer (GCL)
Nerve fiber layer
Cone
Rod
Photoreceptors
Horizontal cell
Bipolar cell
Amacrine cell
Ganglion cell
To optic nerve
Light

Figure 1

1.6 Horizontal Cells

HCs are inhibitory interneurons located in the outer retina that negatively feedback to photoreceptors through lateral inhibition, a negative feedback loop crucial for generating spatial discrimination, edge detection, and colour opponency (Thoreson & Mangel, 2012). Despite extensive research on their activity, the specific mechanism of HC feedback remains unclear. However, three main mechanisms have been proposed: (1) an ephaptic mechanism through hemichannels at HC terminals (Byzov & Shura-Bura, 1986; Vroman et al., 2013); (2) HCs release protons to modulate H^+-sensitive Ca^{2+} channels on the PR membrane (Jonz & Barnes, 2007; Jacoby et al., 2012; Barnes et al., 2020); (3) GABA release via Ca^{2+}-dependent vesicular release or Na^+-dependent transport; however, the exact method of GABA release in goldfish HCs remains unclear (Lam et al., 1978; Ayoub & Lam, 1984, 1985; Hirano et al., 2016; Barnes et al., 2020). The GABA and proton release hypotheses were more recently presented as a hybrid model in mammalian retina, suggesting that both mechanisms operate together to produce inhibitory feedback (Barnes et al., 2020).

There are four main subtypes of HCs in teleosts (H1-H4) and they are ordered by increasing distance from the outer retinal layer, increasing dendritic field, and decreasing size of the cell body (Country & Jonz, 2022; Stell & Lightfoot, 1975). Notably, H1 cells are one of the most abundant cell types in the retina (Country & Jonz, 2021) and are also the only subtype that has been found to store and release GABA during feedback modulation in goldfish and crucian carp (Marc et al., 1978).

1.7 iGluR and Ca^{2+} Regulation in HCs

In darkness, photoreceptors are tonically depolarized and continuously release glutamate, which depolarizes HCs and modulates bipolar cell (BC) responses depending on the receptor subtype (Hoon et al., 2014; Miller & Schwartz, 1983). Glutamate binding to receptors at the HC membrane triggers Ca^{2+} influx through ionotropic glutamate receptors (iGluR) as well as depolarization of the cell. Cell depolarization results in the opening of VGCC channels, facilitating a greater influx of Ca^{2+} into the cell (Linn & Christensen, 1992; Tachibana, 1983). An increase in Ca^{2+} influx triggers the release of even more Ca^{2+} ions from intracellular stores within the ER via ryanodine receptors (RyR), a process known as Ca^{2+}-induced Ca^{2+} release (CICR) (Huang et al.., 2004). Given the amount of Ca^{2+} entering the cell, HCs have multiple mechanisms in place to regulate intracellular $[Ca^{2+}]_i$ when it surpasses the homeostatic range. Ca^{2+} can be extruded outside the cell by the plasma membrane Ca^{2+}-ATPase (PMCA) and the Na^+/Ca^{2+} exchanger (NCX), pumped back into the ER through the sarcoplasmic/endoplasmic reticulum Ca^{2+}-ATPase (SERCA) or can be stabilised through cytosolic Ca^{2+} buffering (reviewed in Country & Jonz, 2017).

iGluR are permeable to ions, such as Na^+ and Ca^{2+}, but this can vary between species and differ in permeability, depending on the presence of certain subunits. In goldfish HCs, NMDARs, Ca^{2+}-permeable and Ca^{2+}-impermeable AMPARs, and kainite receptors can all be found on the plasma membrane (reviewed in Country & Jonz, 2017). AMPARs are composed of a combination of subunits from GluA-GluA4. The Ca^{2+} permeability of AMPARs depends on the presence of the GluA2 subunit. AMPARs composed of subunits without GluA2 are permeable to Ca^{2+} but this difference is dependent on the editing of a single amino acid site, where glutamine is converted to arginine (Wright & Vissel, 2012; Peng et al., 2006; Liu & Cull-Candy, 2000).

NMDARs are ligand-gated ion channels that are composed of seven subunits of GluN1, four subunits of GluN2 and two subunits of GluN3, which all can be arranged to give these channels unique biophysical properties (Paoletti et al., 2013). NMDARs are permeable to Ca^{2+} and open following activation of AMPARs. This results in depolarization of the cell membrane and removal of Mg^{2+} ion that plugs NMDARs allowing for the propagation of the action potential (Mayer et al., 1984).

In light of the evidence that hypoxia-tolerant species such as goldfish, carp, and turtles employ pathways to reduce neuronal excitability, as well as the previous work done in our lab demonstrating that mK_{ATP} activation contributes to hypoxia tolerance and intracellular Ca^{2+} signalling in goldfish HCs, this thesis investigates how iGluR activity is altered during hypoxia and whether this response depends on mK_{ATP} activation and intracellular Ca^{2+} release. By understanding this link, we aim to present a potential adaptive signalling mechanism that enables HCs to supress neural activity and maintain cell function to evade excitotoxicity during metabolic stress.

1.8 Thesis Objectives

Building on the hypoxia-induced rise in $[Ca^{2+}]_i$ observed in HCs observed by Nagy-Watson & Jonz (2025), the present study investigates two possible neuroprotective mechanisms in the goldfish retina. The first hypothesis is that hypoxia supresses iGluR activity in the plasma membrane of HCs through the activation of mK_{ATP} channels and a Ca^{2+} signalling pathway. The second hypothesis proposes that the opening of mK_{ATP} channels triggers Ca^{2+}-induced GABA release from HCs as a form of inhibitory feedback to reduce metabolic demand. By comparing

these mechanisms, this thesis aims to clarify which process underlies hypoxia tolerance in the goldfish retina and how excitatory signalling is regulated during metabolic stress.

To address these hypotheses, we set out the following objectives:

- Determine whether hypoxia suppresses iGluR-activated currents in HCs compared to glutamate-activated currents in normoxia.
- Test whether this suppression is dependent on the activation of mK_{ATP} channels.
    - If the suppressed response is dependent on mK_{ATP} activity, we predict that the response will be abolished during pharmacological inhibition of mK_{ATP} channels.
- Assess whether the suppression of iGluR activity during hypoxia is mediated by cytosolic Ca^{2+} signalling.
    - If ryanodine receptors, or the mitochondrial Ca^{2+} uniporter are involved in this mechanism, we predict that the suppressed response will be abolished during the pharmacological inhibition of these channels.
- Assess whether glutamate in the presence of hypoxia promotes GABA release from HCs via Ca^{2+}-mediated GABA release.
    - If HCs release greater amounts of GABA during hypoxia compared to normoxic conditions (in the presence of glutamate), this would indicate that HCs employ GABA release as a neuroprotective strategy.

By comparing these pathways, the present thesis aims to determine whether suppression of iGluR activity or Ca^{2+}-dependent GABA release represents the primary neuroprotective mechanism in goldfish retina. Clarifying these processes will improve our understanding of how

retinal neurons regulate excitability under metabolic stress and may contribute to broader strategies aimed at protecting hypoxia-intolerant systems, including the mammalian retina during ischemia.

2. METHODS

2.1 Ethical Approval

Animal care procedures were approved by the University of Ottawa Animal Care and Veterinary Services (protocol BL-1760) and followed the guidelines set by the Canadian Council on Animal Care. Adult common goldfish (*Carassius auratus*) were obtained from the commercial supplier Mirdo Importations Canada (Montreal, QC, Canada) and housed in the University of Ottawa Laboratory for the Physiology and Genetics of Aquatic Organisms. Fish were kept in 170 L tanks with a continuous flow of fresh, aerated and dechloraminated water held at 18°C. A 12h light:12h dark photoperiod was maintained. Prior to experimentation, goldfish were dark adapted for at least 1 h before being euthanized. All datasets presented in this study were obtained from recordings of cells collected from both male and female individuals of different ages.

2.2 Isolated Cell Preparation

HCs isolation followed a similar protocol to Jonz and Barnes (2007). Adult common goldfish were anesthetized by a sharp blow to the head, then swiftly decapitated and pithed. Eyes

were enucleated and placed in ice-cold, Ca^{2+}-free Ringer's solution composed of the following (in mM): 120 NaCl, 2.6 KCl, 1 $NaHCO_3$, 0.5 NaH_2PO_4, 1 sodium pyruvate, 4 HEPES, and 16 glucose, adjusted to pH 7.8 with NaOH. The optic nerve was cut, and the sclera and lens were removed to provide access to the retinal layer. Retinas were then extracted from the eyecups and transferred to L-15 solution (made of 70% Leibovitz's L-15 medium and 30% Ca^{2+}-free Ringer's solution) containing 100 U mL^{-1} hyaluronidase (Cat. No. H3506, Sigma, Mississauga, ON, Canada) for 20 min at room temperature to eliminate excess vitreous material. Retinas were then rinsed three times in fresh L-15 for 3 min per rinse and placed in L-15 solution containing 7 U mL^{-1} papain (Cat. No. 3126, Worthington Biochemical Corporation, Lakewood, NJ, USA) and 2.5 mM L-cysteine (Cat. No. C7352, Sigma) for 40 min at room temperature to aid in cell separation. The tissue was then cut into small pieces (~2-4 mm^2) and gently triturated in 1 mL of L-15 to mechanically dissociate the cells. The resulting cell suspension was transferred to a 35 mm Petri dish (Corning Inc. Bedford, MA, USA) and left to settle for 15 min before beginning patch-clamp experiments.

2.3 Electrophysiology

Patch-clamp recordings were performed using the perforated-patch configuration. Electrodes were pulled on the day of recording from borosilicate capillary glass tubes (Cat. No. TW150-3, World Precision Instruments) on a vertical micropipette puller (Model PC-100, Narishige CO. Ltd, Japan) and fire polished with a microforge (model MF-830, Narishige) to a resistance of 6-12 MΩ. Electrode tips were filled with intracellular solution containing (in mM): 10 NaCl, 120 KCl, 2 $MgCl_2$, and 10 HEPES with pH adjusted to 7.4 with KOH. Electrodes were then backfilled with a solution of amphotericin B at a working concentration of 10–62.5 µg/mL.

Only cells with a stable membrane seal of >1 GΩ were used. Isolated cells were plated into a 35 mm Petri dish fitted with a perfusion chamber. Throughout recordings, cells were continuously superfused at a rate of at ~1 mL min^{-1} using a gravity-driven perfusion system. A peristaltic pump simultaneously removed the solution at the same flow rate to prevent fluctuation of fluid level in the dish and maintain a positive meniscus.

All protocols were preformed with pClamp 7 software, an Axopatch 1D amplifier, and a Digidata 1440A (Axon Instruments, Sunnyvale, CA, USA). All cells were clamped at a holding potential of –60 mV. Macroscopic membrane currents were recorded using voltage-ramp protocols in which the membrane potential (V_m) was gradually depolarized from –120 mV to +100 mV over 1 s. Additionally, gap-free recordings were also conducted to monitor spontaneous current activity over extended periods of time (30–45 min). Throughout these recordings, various drugs were applied through perfusion and their effects on membrane current was recorded. Membrane capacitance (C_m) was measured with pClamp 7.

2.4 Experimental Procedures and Solutions

After plating, cells were given 10-15 min to reach the bottom of the dish before any patch-clamping experiments began. Cells were washed with extracellular solution (ECS) in mM: 120 NaCl, 5 KCl, 2.5 $CaCl_2$, 2 $MgCl_2$, 10 HEPES, and 10 glucose with pH adjusted to 7.8 with NaOH, for a few minutes before recording to remove any debris. In all experiments HCs were treated with normoxic ECS for a few minutes to establish a stable baseline recording. Hypoxic exposure lasted no longer than 2 min during voltage-ramp protocols, and 15 min or longer during gap-free recordings.

Hypoxic solutions were prepared by bubbling solution reservoirs with 100% N_2 for a minimum of 20 min prior, resulting in a recording solution with a PO_2 of approximately 25 mmHg (Jonz et al., 2004). Control solutions were bubbled with air for the same duration. HCs were treated with glutamate for 2 min at three time points: (1) in normoxic conditions as a control, (2) after hypoxic exposure, and (3) following a washout period. Similar experiments were conducted with normoxic ECS to serve as a sham control. Glutamate (100 μM; Cat. No. 49621, Sigma), and ruthenium red (400 nM; Cat. No. 1439, Tocris) were dissolved in double-distilled water. Ryanodine (20 μM; Cat. No. 1329, Tocris), glibenclamide (100 μM; Cat. No. G0639, Sigma), BAPTA-AM (50 μM; Cat. No. A1076, Sigma) and diazoxide (100 μM; Cat. No. D9035, Sigma) were dissolved in dimethyl sulfoxide (DMSO, Cat. No. D8418), which never surpassed a final concentration of 0.25% v/v. At this concentration, DMSO had no effect on membrane currents. The concentrations of all solutions used are summarized in Table 1.

Table 1. Composition of extracellular solutions. Unless stated otherwise, pH was adjusted to 7.8 with NaOH for all solutions.

	Solutions and chemical concentrations (in mM)							
Chemical	ECS	High K^+ ECS	ECS + BAPTA -AM	ECS + Glutamate	ECS + Glibenclamide	Glibenclamide + Glutamate	Ruthenium Red + Glutamate	Ryanodine + Glutamate
NaCl	120	85	120	120	120	120	120	120
KCl	5	40	5	5	5	5	5	5
$CaCl_2$	2.5	2.5	2.5	2.5	2.5	2.5	2.5	2.5
$MgCl_2$	2	2	2	2	2	2	2	2
HEPES	10	10	10	10	10	10	10	10
Glucose	10	10	10	10	10	10	10	10
Glutamate	-	-	-	0.1	-	0.1	0.1	0.1
Glibenclamide[1]	-	-	-	-	0.1	0.1	-	-
Ruthenium Red	-	-	-	-	-	-	0.0004	-
Ryanodine[1]	-	-	-	-	-	-	-	0.2
BAPTA-AM[1]	-	-	0.05	-	-	-	-	-

1. Dissolved in DMSO to a final concentration of 0.25% v/v.

2.5 GABA Release Experimental Procedures and Solutions

Retinas were removed and treated with enzymes for dissociation (as described above), then rinsed an additional 3 times in ECS. The experimental design ensured that each goldfish contributed to 3 equal samples across treatment groups to minimize variability. These samples were then assigned to one or more of the following six treatment conditions: 1) control (ECS), 2) glutamate, 3) high K^+, 4) hypoxia, 5) hypoxia + glutamate, or 6) glutamate + diazoxide. The specific combination of treatments varied depending on the experimental setup. In some cases, all three samples received different treatments. In other cases, one or more samples received the same treatment. For example, one fish might have two samples treated with hypoxia and glutamate and one with glutamate alone. Each retina was then triturated to mechanically dissociate the cells. Cells were placed in a 2 mL treatment solution of high K^+ ECS (prepared by equimolar substitution of NaCl with 35 in mM KCl), which served as a positive control by depolarizing HCs to induce GABA release. Cells were exogenously treated with glutamate and/or diazoxide, which were diluted in ECS to a final concentration of 100 μM. The mK_{ATP} agonist diazoxide was first dissolved in DMSO ensuring the final concentration remained below 0.25% v/v (Country & Jonz, 2021; Nagy-Watson & Jonz, 2025).

The cell treatment suspensions were transferred into 35 mm culture dishes and placed in an atmosphere-controlled incubator (Forma 3130, ThermoFisher Scientific, Ottawa, ON, Canada) at 22-24°C. Experimental samples were subjected to hypoxic conditions (P_{O2} = 15 mmHg) for 1 h, while control samples remained in normoxia for the same duration. After incubation, cell suspensions from each dish were moved into 15 mL Falcon tubes and centrifuged at 1100 RPM for 5 min, or until a pellet formed. The supernatant was collected, passed through a 0.2 μm syringe filter, and transferred into a microcentrifuge tube. Finally, the

samples were stored at -20 °C and sent to the Carleton Mass Spectrometry Centre at Carleton University to test for the presence of GABA using liquid chromatography mass spectrometry (LC-MS) analysis. Chemical analysis was performed entirely by collaborators, Dr. Christian Rosales and Dr. Jeffrey Smith. Samples were dried to completeness using a stream of N_2 and reconstituted in an aqueous caffeine diluent internal standard (IS) mixture (0.5 μM) prior to LC-MS analysis. Standard samples were reconstituted in the same volume of IS diluent as the original sample aliquot amount, whereas saline culture media and goldfish retina supernatant samples were diluted 5-fold to mitigate matrix effects. Upon immediate analysis, all samples were stored at -20 °C. An overview of this experimental procedure is shown in Figure 2.

Figure 2. Overview of protocol to detect GABA release from goldfish horizontal cells by mass spectrometry. Retinas were extracted from goldfish and mechanically dissociated after incubating with 100 U mL^{-1} hyaluronidase and 7 U mL^{-1} papain. Following dissociation, both retinas were divided into three equal suspensions and then exposed to one of six treatment conditions: (1) control (ECS), (2) glutamate, (3) high K^+ (positive control), (4) hypoxia, (5) hypoxia + glutamate, or (6) glutamate + diazoxide. After a 1 h incubation period under normoxic or hypoxic conditions ($PO_2 \approx 15$ mmHg), cells were transferred to centrifuge tubes (labeled 1–3 here for simplicity), centrifuged, filtered, and stored at –20 °C for subsequent GABA quantification by mass spectrometry (see Methods for details).

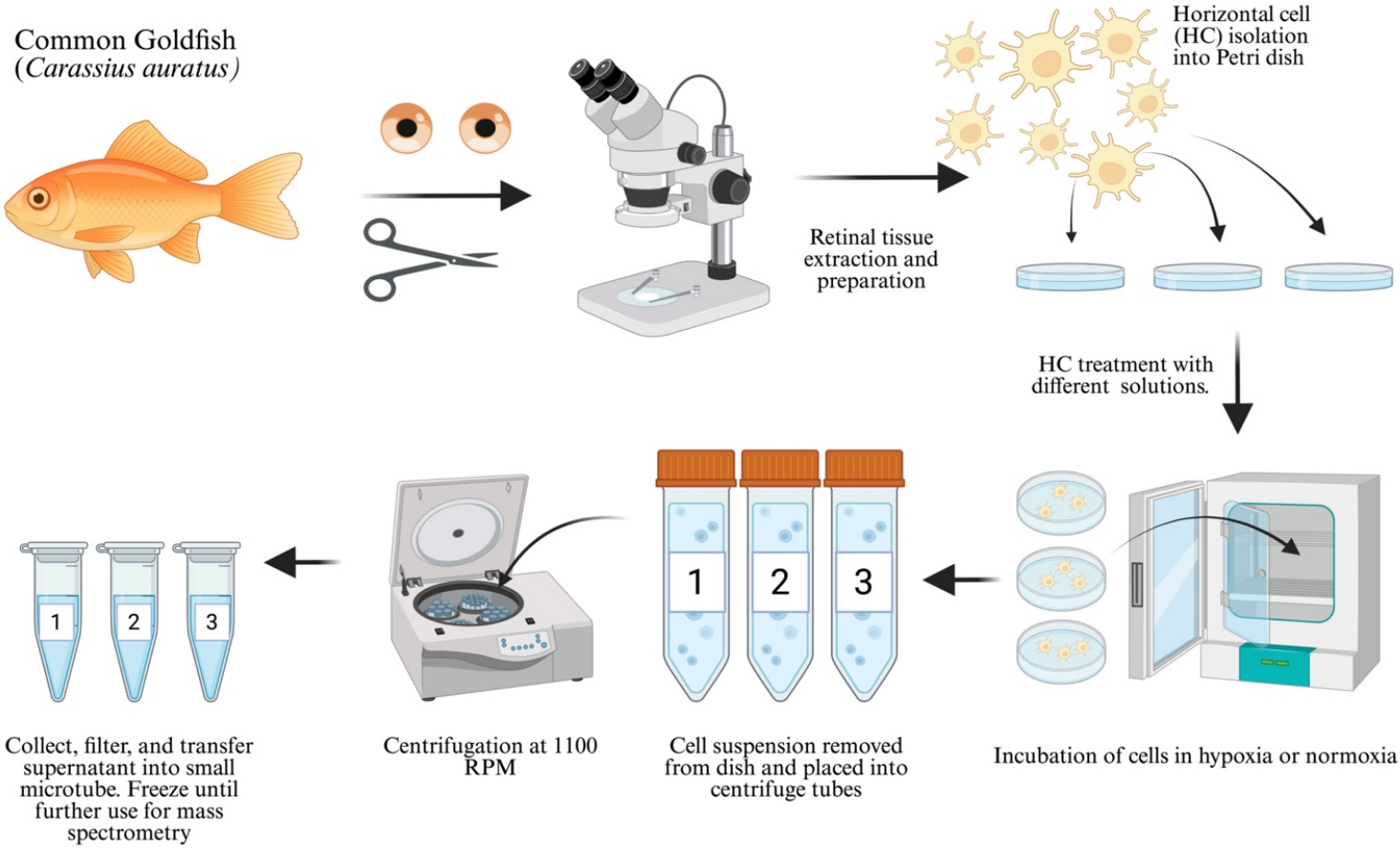
Common Goldfish
(*Carassius auratus*)
Retinal tissue extraction and preparation
Horizontal cell (HC) isolation into Petri dish
HC treatment with different solutions.
Incubation of cells in hypoxia or normoxia
Cell suspension removed from dish and placed into centrifuge tubes
Centrifugation at 1100 RPM
Collect, filter, and transfer supernatant into small microtube. Freeze until further use for mass spectrometry
1
2
3

Figure 2

2.6 Materials for Chemical Analysis, Reversed-Phase Liquid Chromatography, and ESI-Multiple Reaction Monitoring (MRM) Analysis

We developed a procedure for the detection of GABA in the supernatant samples using mass spectrometry (Rosales et al., 2025). GABA, caffeine, and HBF_4•Et_2O were purchased from Sigma-Aldrich (St. Louis, MO, USA). LC-MS grade water with 0.1% formic acid, acetonitrile (ACN) with 0.1% formic acid, and methanol were purchased from Fisher Scientific (Hampton, NH, USA). Potassium hydroxide and diethyl ether were purchased from Caledon Laboratories Ltd. (Georgetown, ON, Canada). A sample volume of 20 µl was injected into a Dionex Ultimate 3000 HPLC (Thermo Fisher Scientific, Waltham, MA, USA) and separated on an Agilent Eclipse plus C18 3.5 µm column (4.6 x 100 mm) at room temperature. At a constant flow rate of 0.6 mL/min, analytes were eluted using eluent A (water + 0.1% formic acid) and eluent B (acetonitrile + 0.1% formic acid) over a 10.5 min gradient [0.0-1.0 min, 0.5% (B); 5.0 min, 50% (B); 5.1-8.0 min, 100% (B); 8.1-10.5 min, 0.5% (B)]. HPLC eluent entered a QTrap 4000 hybrid triple quadrupole linear ion trap MS (Sciex, Framingham, MA, USA), analyzing all samples in positive ion mode. The Turbo Spray ion source parameters were as follows: curtain gas of 20, high collision gas, 5000 V ionization voltage, temperature of 375 °C, ion source gas 1 of 30, and ion source gas 2 of 10. All samples were analyzed using optimized MRM transitions at 20 Hz (50 ms), with each analyte having a transition pair for semi-quantitation and validatory identification (Table 2).

Table 2. Optimized MRM transition pairs for all unmodified, and internal standard (IS).

TrEnDi-derivatized GABA is denoted with square brackets and a "Tr" superscript (e.g., $[Analyte^{Tr}]^{+}$).

Analyte	MRM Transitions (m/z)	DP (V)	EP (V)	CE (V)	CXP (V)
GABA	104.3 → 87.2	28	10	14	15
	104.3 → 69.1	32	8	21	14
Caffeine (IS)	195.1 → 138.1	75	7	28	10
	195.1 → 110.1	75	7	28	10

2.7 Data Analysis

All electrophysiological data were analyzed using pClamp 7 and GraphPad Prism 7.0. Current density was calculated by dividing the cell's measured peak current by the membrane capacitance (pA/pF), allowing for normalization across cells of varying size. Normality was tested using the D'Agostino & Pearson test, and most datasets were not normally distributed. As a result, data are presented as medians with interquartile ranges, except for one dataset (Fig. 5) that met normality criteria and is shown as mean values ± SEM. Differences in peak current density were compared using the Wilcoxon signed rank test, and ramp difference currents were analysed with the Mann-Whitney U test. The normally distributed dataset was analysed using a one-way repeated measures ANOVA with Bonferroni multiple comparisons and the Geisser Greenhouse correction. All columns were compared with each other with a significance level of 0.05. To test whether hypoxia affected GABA release from HCs, we measured extracellular GABA concentrations ($[GABA]_e$) across several experimental conditions. $[GABA]_e$ was

recorded using mass spectrometry after cells had been incubated under hypoxic or normoxic conditions. GABA data were presented as mean ± SEM and analyzed using either a Mann Whitney U test for pairwise comparisons or a Kruskal-Wallis test with Dunn's *post hoc* correction for multiple group analyses.

3. RESULTS

3.1 Prolonged Application of Hypoxia Decreased iGluR Activity

All cells presented in this study were recorded using perforated patch clamp electrophysiology. Recordings were obtained form 54 HCs collected from 40 male and female goldfish of various ages. To assess the effects of hypoxia on iGluR activity, inward Na^+ currents evoked by glutamate receptor activation were recorded to measure changes in current responses to glutamate in the presence and absence of hypoxia. Current-voltage (*I-V*) relationships were taken before and immediately after a 2 min exposure to either hypoxic or normoxic conditions in the presence of 100 μM glutamate. A washout trace was included in both conditions to confirm the return to baseline following glutamate application. In both normoxia and hypoxia, glutamate-activated currents demonstrated similar *I–V* profiles (Fig. 3A, B; $N = 8$). Glutamate application produced a significant inward current under both conditions, with median peak current densities of -3.30 [-8.04, -2.59] pA/pF ($P = 0.0039$) in normoxia and -3.27 [-7.80, -2.06] pA/pF ($P = 0.0039$) in hypoxia at -60 mV (Fig. 3C). Difference currents for glutamate activation between normoxia and hypoxia showed a marginal reduction with median values of -2.99 [-6.97, -2.41] pA/pF and -2.60 [-5.95, -1.54] pA/pF, respectively, though this effect was not statistically significant (Fig. 3D; $P = 0.4418$).

After establishing the effects of brief hypoxic exposure on HCs had no effect on iGluR, we next examined if prolonged hypoxia affects these responses. Cells were clamped at -60 mV and current activity was monitored during continuous hypoxic or normoxic exposure. In both conditions, three 2-min glutamate applications were delivered with a 5-min washout period between each bout to allow responses to return to baseline before proceeding with the next treatment. Under hypoxia, no significant difference was detected between the first and second glutamate application. However, after approximately 15 min of hypoxic exposure, the third glutamate response was significantly reduced compared to the first, causing a 10.53% decrease in median peak current density (Fig. 4A, B; $N = 9$; P = 0.0059). Median peak current densities in hypoxia were -4.18 [-5.52, -3.09] pA/pF for bout 1, -3.64 [-5.03, -2.93] pA/pF for bout 2 and -3.74 [-3.80, -2.02] pA/pF for bout 3. By contrast, normoxic recordings showed stable responses across all three applications for all cells, with no significant difference between the first and the third bouts (Fig. 4C, D; $N = 6$; P = 0.1563). Median peak current densities in normoxia were -4.00 [-4.45, -2.19] for bout 1, -3.93 [-4.80, -2.37] pA/pF for bout 2, and -3.98 [-5.00, -2.36] pA/pF for bout 3.

With the hypoxia-induced suppression of glutamate-activated inward current established, we wanted to understand whether these effects were reversible. Cells were exposed to three glutamate applications, each at a specific timepoint: the first under normoxic conditions as a control, the second after 15 min of hypoxia, and the third following 10 min of reoxygenation (Fig. 5A). Under normoxia, the first glutamate application produced a strong current response with a peak current density of –4.53 ± 0.56 pA/pF on average (Fig. 5B; $N = 8$). After 15 min of hypoxic exposure, mean peak current density was reduced to –3.81 ± 0.49 pA/pF, resulting in a 15.9% decrease in mean peak current density relative to the first bout (P = 0.0312). Following 10

min of reoxygenation, the third glutamate response was recorded at –3.98 ± 0.56 pA/pF on average, which was not significantly different from the second bout indicating only minor recovery. In all cells recorded, hypoxia significantly lowered iGluR responses after 15 min, but reoxygenation for 10 min did not recover current activity to control levels.

3.2 Blocking Mitochondrial K_{ATP} Channels Abolished the Hypoxia-Induced Reduction in iGluR Activity.

To determine if the suppression of iGluR activity during prolonged hypoxia is dependent on mK_{ATP} channel activation, 100 μM of glibenclamide was coapplied with hypoxia. The same experimental protocol as in Figure 4 was applied with three 2-min glutamate applications separated by 5-min washout periods. In the presence of glibenclamide, hypoxia did not reduce glutamate current amplitude (Fig. 6A). Summary data showed that median peak current density during the first glutamate application was -3.42 [-4.79, -2.68] pA/pF and remained stable during the second (-3.45 [-4.95, -2.78] pA/pF) and third (-3.45 [-4.53, -2.62] pA/pF) applications (Fig. 6B; $N = 6$). Statistical analysis revealed no significant difference in current density across bouts ($P = 0.1563$), suggesting that blocking mK_{ATP} channels abolished the hypoxia-induced suppression of iGluR.

3.3 Hypoxia-Dependent Reduction in iGluR Activity was Inhibited by Blocking Intracellular Stores.

To test whether the hypoxic suppression of iGluR activity depended on intracellular Ca^{2+} signaling, we blocked Ca^{2+} uptake into the mitochondria, which would lead to an increase in

$[Ca^{2+}]_i$. We targeted the MCU using 400 nM ruthenium red. Under hypoxia, glutamate-evoked currents remained stable across all three bouts (Fig. 7). Median peak current density was -3.68, [-6.21, -2.77] pA/pF during the first glutamate application and -3.94 [-5.29, -2.24] pA/pF for the third, with no significant difference across all three bouts ($P = 0.0781$; $N = 6$). Although a small reduction in current amplitude was observed, blocking the MCU increased $[Ca^{2+}]_i$ to a level that likely prevented the suppression of glutamate-evoked currents observed by the third bout under hypoxia.

Next, we blocked Ca^{2+} release from the ER by applying 20 μM ryanodine. These results are preliminary, as only two cells were successfully recorded with this protocol. In both cases current amplitudes remained stable throughout. Median current density was -5.53 [-8.65, -2.42] pA/pF in the first bout and -5.46 [-8.49, -2.43] pA/pF in the third, suggesting that blocking Ca^{2+} release through ryanodine receptors abolishes the hypoxia-induced suppression in the presence of glutamate (Fig. A1; $N = 2$). As additional preliminary evidence, we used pre-treatment with 50 μM of the Ca^{2+} chelator, BAPTA-AM, for 20 min to reduce free $[Ca^{2+}]_i$, followed by a 10 min wash in ECS before beginning recording. In the one cell, glutamate current amplitudes showed no reduction across all bouts (Fig.A2), supporting the conclusion that controlled intracellular Ca^{2+} release is required for the hypoxic suppression of iGluR activity.

These results, together with our preliminary findings, suggest that mK_{ATP} channel activation triggers a Ca^{2+}-dependent pathway that mediates downregulation of iGluRs in response to hypoxia in goldfish HCs.

3.4 Increased $[Ca^{2+}]_i$ Did Not Contribute to GABA Release during Hypoxia

The data presented from chemical analysis are derived from 29 dishes of HCs, with each dish representing an individual sample. All 30 samples were collected from 11 goldfish, with each goldfish (2 retinas) yielding 3 dishes. Extracellular GABA concentration ($[GABA]_e$) was measured across several experimental conditions using mass spectrometry after cells had been incubated under hypoxic or normoxic conditions to assess GABA release. As shown in Fig. 8A, both glutamate and high K^+ solution increased $[GABA]_e$ to 311.50 ± 22.92 and 806.50 ± 135.10 nM, respectively, with high K^+ solution giving the greatest difference and resulting in a 10.25-fold increase compared to control (N = 8, P = 0.0373). These findings confirm sensitive detection of GABA release from depolarized HCs using mass spectrometry. The chromatogram from the high K^+ sample is provided in Figure 8.

To assess the effect of hypoxia alone on GABA release, cells were incubated under normoxic or hypoxic conditions for 1 h. Mean $[GABA]_e$ was 113.80 ± 4.85 nM in normoxia and 97.85 ± 11.90 nM under hypoxia, with no significant difference between treatments (Fig. 8B; N = 5; P = 0.2000). Co-application of glutamate with hypoxia yielded a mean $[GABA]_e$ of 345.40 ± 45.56 nM, which was not significantly different compared to $[GABA]_e$ from cells treated with glutamate under normoxic conditions (462.10 ± 61.77 nM; Fig. 8C; P = 0.1234; N = 11).

Activation of mK_{ATP} channels with 100 μM diazoxide in the presence of glutamate also did not affect GABA release. Mean concentrations were 534.20 ± 86.71 nM for glutamate alone compared to 553.50 ± 41.62 nM for glutamate and diazoxide with no significant difference detected between both groups (Fig. 8D; P = 0.5000; N = 6).

Figure 3. Acute hypoxia (2 min) did not affect glutamate receptor activity in goldfish horizontal cells. (**A**) Representative voltage-clamp recording from a HC under normoxic conditions. Cells were treated with ECS for 2 min, followed by application of 100 μM glutamate for 2 min, and then a 2 min washout. (**B**) Recording from a different cell under acute hypoxia, following a similar protocol within the same timeframe. In both conditions, glutamate induced an increase in inward current at resting membrane potentials. (**C**) Summary data of current density at -60 mV before, during, and after glutamate applications under normoxia (N = 8 from 6 fish; P = 0.0039) and hypoxia (N = 8 from 5 fish; P = 0.0039), showing significant increase in inward currents in both conditions (Wilcoxon test). (**D**) Difference currents of glutamate-activated currents between normoxic and hypoxic responses, showing no significant difference in amplitude change between the two conditions (Mann-Whitney U test; P = 0.4418). Data are presented as medians with interquartile range.

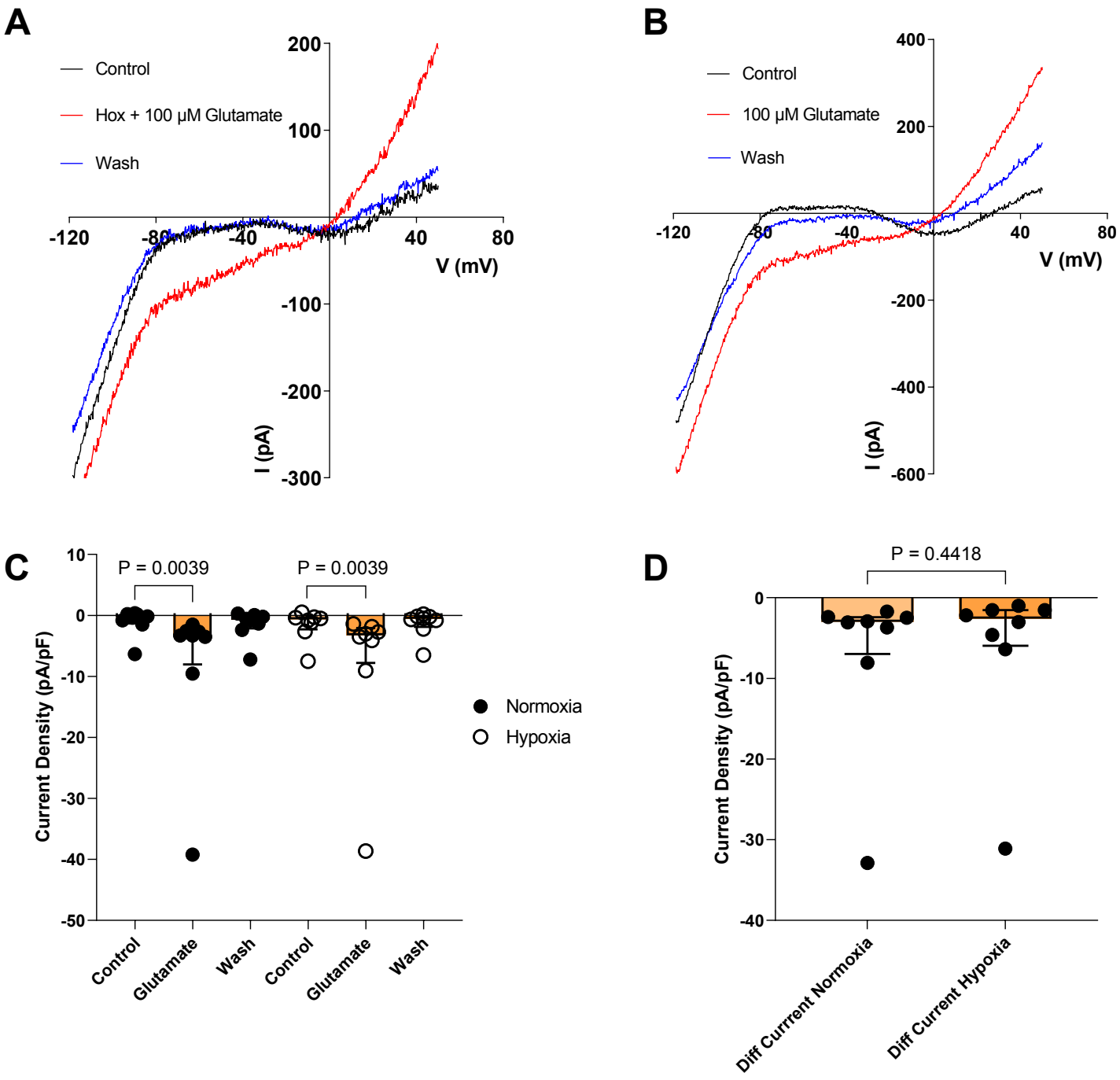
A
Control
Hox + 100 µM Glutamate
Wash
200
100
-100
-200
-300
-120
-80
-40
40
80
V (mV)
I (pA)
B
Control
100 µM Glutamate
Wash
400
200
-200
-400
-600
-120
-80
-40
40
80
V (mV)
I (pA)
C
P = 0.0039
P = 0.0039
Current Density (pA/pF)
10
0
-10
-20
-30
-40
-50
Normoxia
Hypoxia
Control
Glutamate
Wash
Control
Glutamate
Wash
D
P = 0.4418
Current Density (pA/pF)
0
-10
-20
-30
-40
Diff Currrent Normoxia
Diff Current Hypoxia

Figure 3

Figure 4. Prolonged hypoxia suppressed iGluR currents in HCs. (**A**) Representative gap-free single-cell recording from a HC clamped at -60 mV and continuously exposed to hypoxia. Cells were treated with three 2-min applications of 100 μM glutamate, each application separated by a 5-min washout with ECS. (**B**) Summary data showing peak current densities for all three glutamate applications under hypoxia ($N = 9$ from 8 fish), with statistical comparison between the first and third bouts showing a significant reduction in current amplitude over time (Wilcoxon test; $P = 0.0059$). (**C**) Representative recording from a cell under normoxia using an identical protocol as in (A). (**D**) Summary data under normoxia ($N = 6$ from 4 fish), showing no significant difference between the first and third bouts (Wilcoxon test; $P = 0.1563$). Each point represents an individual cell. Data are presented as medians with interquartile range.

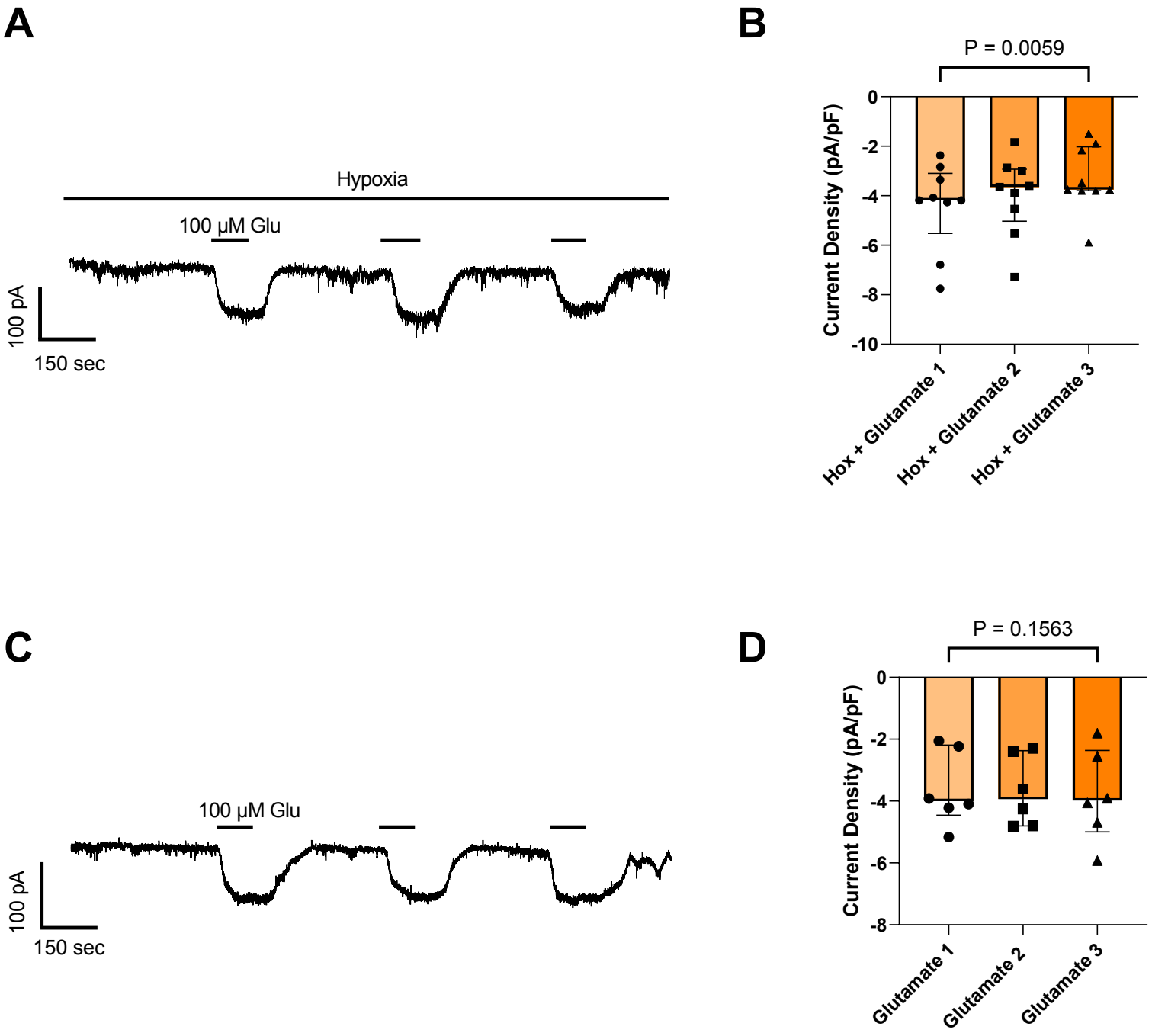
A
Hypoxia
100 µM Glu
100 pA
150 sec
B
P = 0.0059
Current Density (pA/pF)
0
-2
-4
-6
-8
-10
Hox + Glutamate 1
Hox + Glutamate 2
Hox + Glutamate 3
C
100 µM Glu
100 pA
150 sec
D
P = 0.1563
Current Density (pA/pF)
0
-2
-4
-6
-8
Glutamate 1
Glutamate 2
Glutamate 3

Figure 4

Figure 5. Hypoxia-induced suppression of iGluR currents did not recover after 10 min of reoxygenation. (**A**) Representative gap-free single-cell recording from a HC clamped at -60 mV. (**B**) Summary data showing mean peak current densities for all three bouts (N = 8 from 5 fish), statistical comparisons between the first and second bout showed that 15 min of hypoxia significantly lowered current responses (repeated measures one-way ANOVA test; P = 0.0312) but no significant difference was measured between the second and third bouts. Each data point represents an individual cell. Data are presented as mean ± SEM.

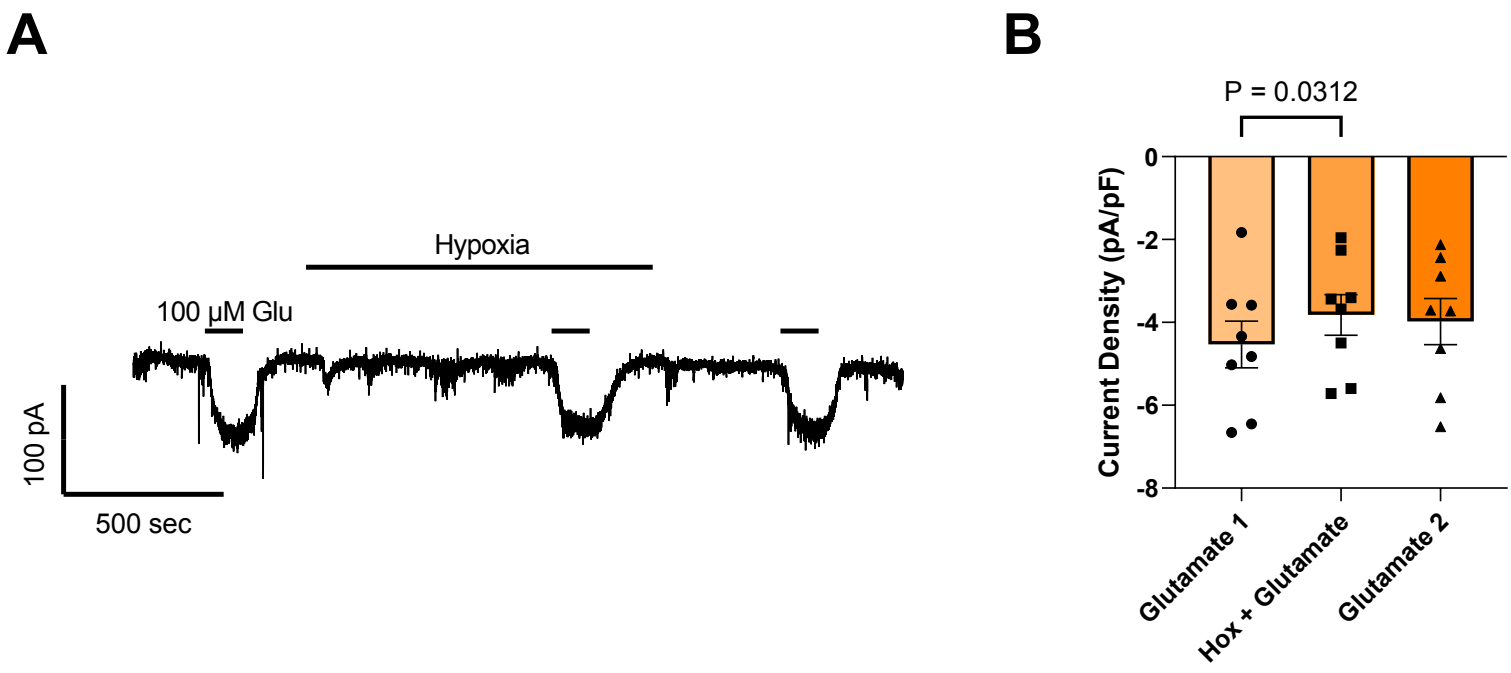
A
Hypoxia
100 µM Glu
100 pA
500 sec
B
P = 0.0312
Current Density (pA/pF)
0
-2
-4
-6
-8
Glutamate 1
Hox + Glutamate
Glutamate 2

Figure 5

Figure 6. Inhibition of mK_{ATP} channels prevented hypoxia-induced suppression of iGluR currents. (**A**) Representative single cell recording clamped at -60 mV showing continuous co-application of hypoxia with 100 μM glibenclamide. Three 2-min applications of 100 μM glutamate were delivered, each separated by a 5-min wash. (**B**) Summary data of mean peak current densities ($N = 6$ from 4 fish). No significance was detected between the first and third application (Wilcoxon test; P = 0.1563). Inhibition of mK_{ATP} channels abolished the reduction in iGluR activity under hypoxia alone. Each point represents an individual cell. Data are presented as medians with interquartile range.

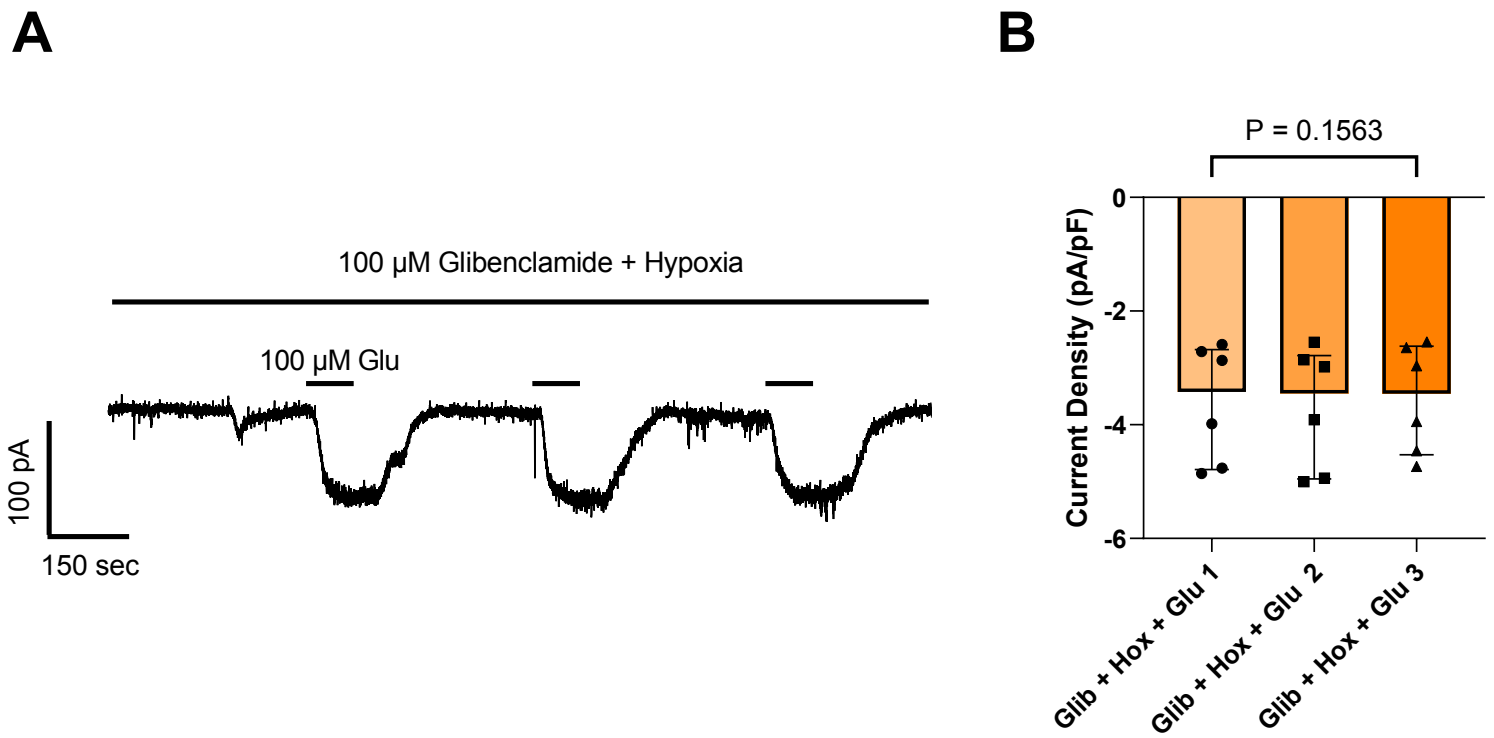
A
100 µM Glibenclamide + Hypoxia
100 µM Glu
100 pA
150 sec
B
P = 0.1563
Current Density (pA/pF)
0
-2
-4
-6
Glib + Hox + Glu 1
Glib + Hox + Glu 2
Glib + Hox + Glu 3

Figure 6

Figure 7. Inhibition of intracellular Ca^{2+} uptake through MCU abolished suppression of iGluR currents during hypoxia. (**A**) Single cell recording of protocol with 400 nM ruthenium red co-applied with 100 μM glutamate. (**B**) Mean current density ± SEM pA/pF showed no significant difference between the first and the third application (N = 6 from 5 fish; Wilcoxon test; P = 0.0781). Data are presented as medians with interquartile range.

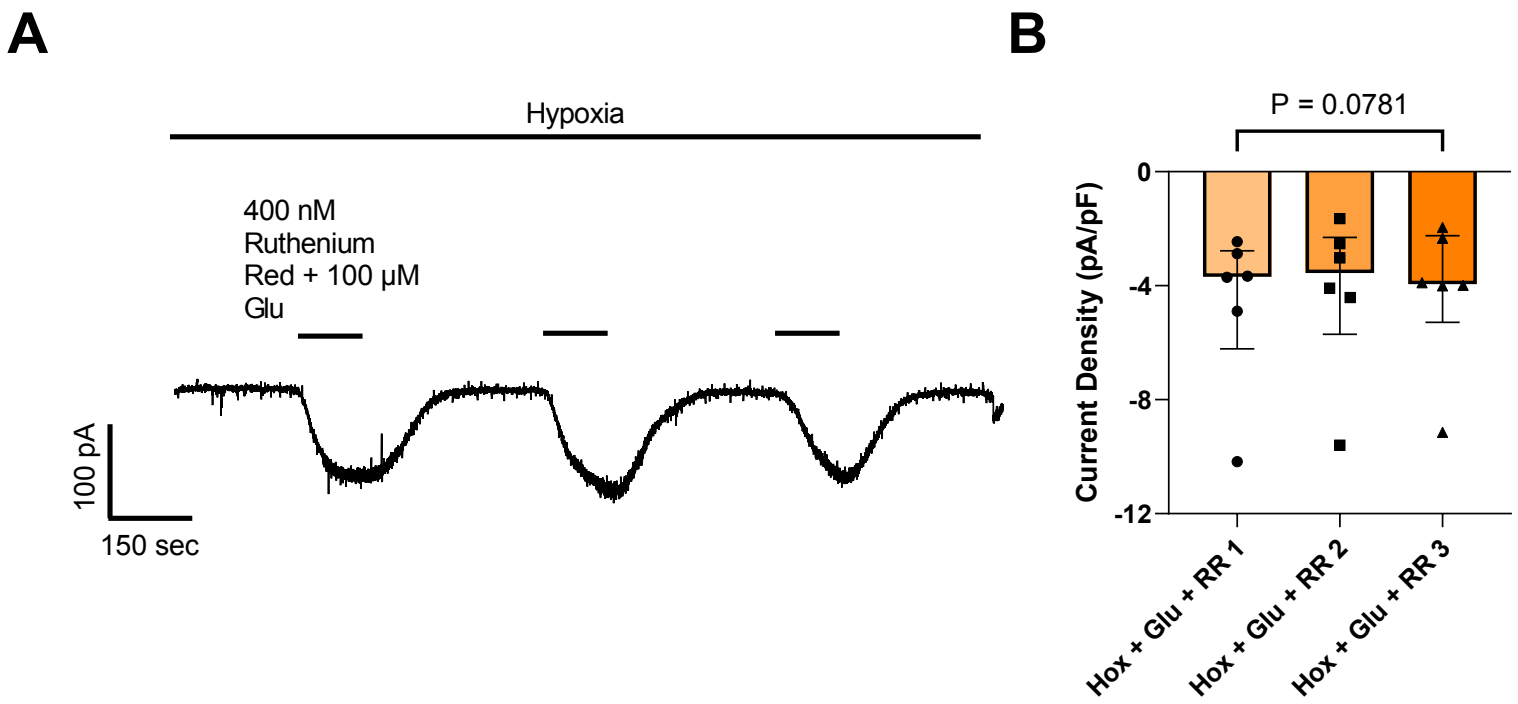
A
Hypoxia
400 nM
Ruthenium
Red + 100 µM
Glu
100 pA
150 sec
B
P = 0.0781
Current Density (pA/pF)
0
-4
-8
-12
Hox + Glu + RR 1
Hox + Glu + RR 2
Hox + Glu + RR 3

Figure 7

Figure 8. Hypoxia did not increase vesicular GABA release from goldfish HCs. (**A**) $[GABA]_e$ measured from isolated HCs following 1 h incubation periods in normoxia, with 100 μM glutamate, or high K^+ ECS. Both glutamate and high K^+ increased $[GABA]_e$, with high K^+ producing the largest response (N = 8 from 3 fish; Kruskal-Wallis test; P =0.0373). (**B**) $[GABA]_e$ in cells incubated for 1 h under normoxia or hypoxia did not show any significant difference (N = 5 from 2 fish; Mann-Whitney U test; P = 0.2000). (**C**) $[GABA]_e$ after 1 h incubation in normoxia or hypoxia co-applied with glutamate. Glutamate applications increased $[GABA]_e$ compared to controls in (B), however GABA release did not differ between hypoxic and normoxic treatment conditions (N = 11 from 4 fish; Mann-Whitney U test; P = 0.1234). (**D**) $[GABA]_e$ in cells exposed to glutamate alone or co-applied with 100 μM diazoxide under normoxia showing no significant effect of mK_{ATP} activation on GABA release (N = 6 from 2 fish; Mann-Whitney U test; P = 0.5000). (**E**) Chromatogram of a GABA K^+ sample analyzed by mass spectrometry. Multiple reaction monitoring (MRM) was used for semi-quantitation of GABA (blue trace) and to verify peak identity (red trace). The y-axis represents intensity (counts per second, cps), and the x-axis shows the retention time (minutes).

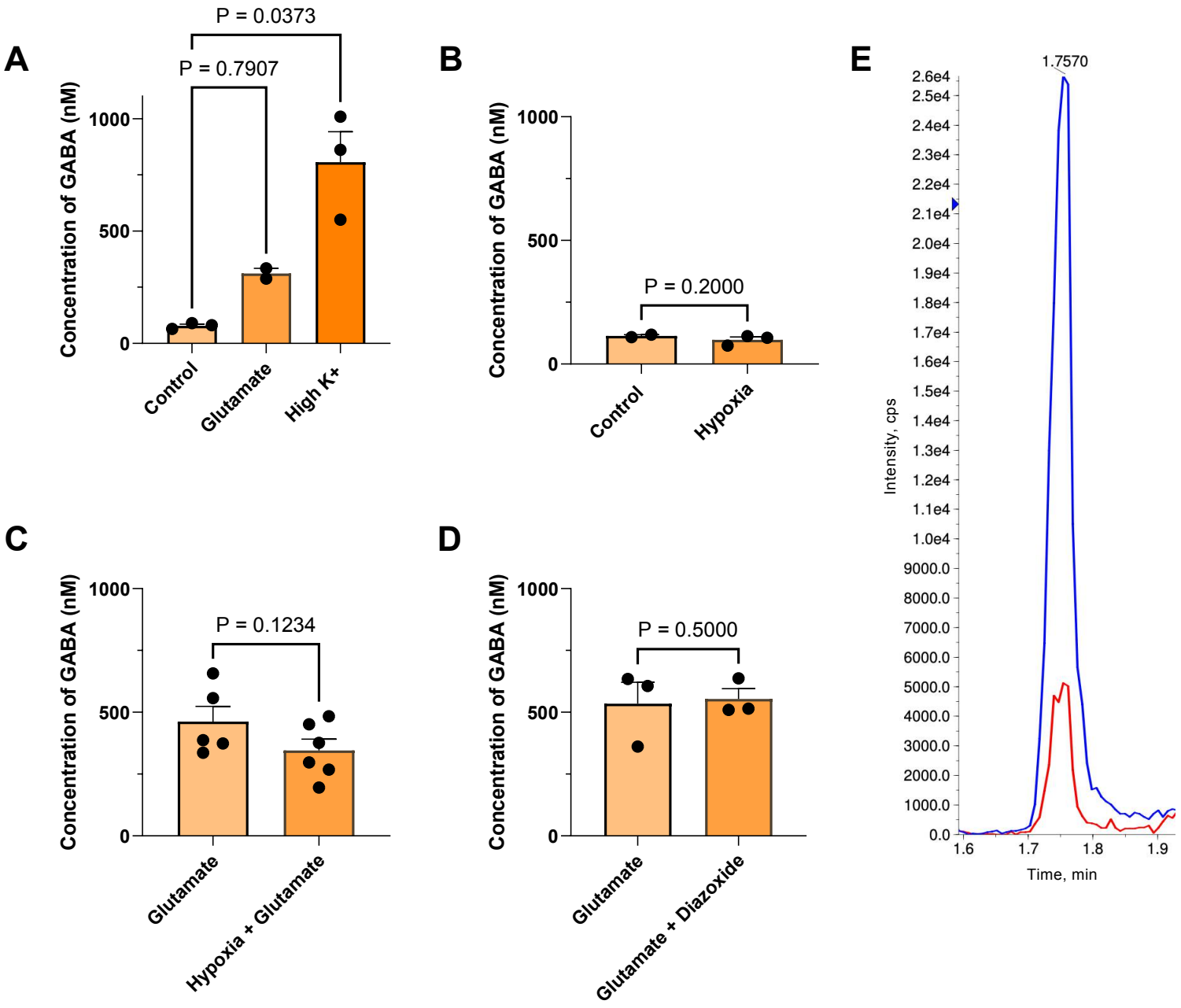
A
P = 0.0373
P = 0.7907
Concentration of GABA (nM)
1000
500
0
Control
Glutamate
High K+
B
Concentration of GABA (nM)
1000
500
0
P = 0.2000
Control
Hypoxia
C
Concentration of GABA (nM)
1000
500
0
P = 0.1234
Glutamate
Hypoxia + Glutamate
D
Concentration of GABA (nM)
1000
500
0
P = 0.5000
Glutamate
Glutamate + Diazoxide
E
1.7570
Intensity, cps
2.6e4
2.5e4
2.4e4
2.3e4
2.2e4
2.1e4
2.0e4
1.9e4
1.8e4
1.7e4
1.6e4
1.5e4
1.4e4
1.3e4
1.2e4
1.1e4
1.0e4
9000.0
8000.0
7000.0
6000.0
5000.0
4000.0
3000.0
2000.0
1000.0
0.0
1.6
1.7
1.8
1.9
Time, min

Figure 8

4. DISCUSSION

4.1 Ionotropic Glutamate Receptor Suppression During Hypoxia

The present study demonstrates that retinal HCs isolated from goldfish display a decrease in glutamate-activated currents over time following 15 minutes of hypoxic exposure. This response likely occurs due to the activation of mK_{ATP} channels and the subsequent release of intracellular Ca^{2+} from stores in the ER, which could be engaging in downstream pathways that are mediating this suppression in the membrane. Building on previous studies from our lab, these results support a model where hypoxia activates mK_{ATP} channels in goldfish HCs in the absence of glutamate, and this activation maintains $[Ca^{2+}]_i$ (Country & Jonz, 2021). In the presence of extracellular glutamate, mK_{ATP} activation during hypoxia paradoxically triggers a modest release of Ca^{2+} from internal stores (Nagy-Watson & Jonz, 2025). This release in Ca^{2+} could be involved in a signaling pathway that ultimately downregulates iGluR in the membrane, thereby conserving energy and contributing to neuroprotective adaption during hypoxic stress (reviewed in Jonz, 2025).

Much of the ATP consumption in the retina is used to maintain ionic gradients across the plasma membrane which is essential for neural signaling (Wong-Riley 2010). When activated, iGluR are permeable to Na^+ and Ca^{2+} (Dingledine et al., 1999; Diamond, 2011), which causes depolarization and opens VGCC. The influx of ions ultimately requires the work of the Na^+/K^+-ATPase and other ion transport mechanisms to restore the cell to resting membrane potential. Thus, each cycle of depolarization and ionic gradient restoration requires a significant amount of energy to maintain, making the retina particularly sensitive to changes in oxygen availability. In hypoxia tolerant vertebrates, one strategy to reduce this burden is by actively downregulating

receptor activity, thereby decreasing ion flux and lowering ATP demand. In crucian carp (*Carassius carassius*), a close relative to the goldfish, responses to light in both the retina and optic tectum are reversibly suppressed during prolonged anoxia. Specifically, response amplitudes decreased by 69% and 75% respectively after 38 min of anoxia and by 90% after 1 h (Johansson et al., 1997). Similarly, Wei & Yang (1997) reported that cone- and rod-driven HCs in crucian carp show a reduction in response amplitude to 76% and 55% from the controls respectively after 10 min of hypoxia. Together, these findings demonstrate that iGluR activity in HCs is downregulated during hypoxia and that this suppression develops gradually over time rather than occurring immediately when oxygen levels drop.

The present study reports no significant difference in glutamate-evoked current amplitude during acute hypoxia (~2 min) compared with normoxic controls. In both conditions, glutamate induced inward current in all recorded HCs, confirming its well-established role as the primary excitatory neurotransmitter in the retina (Massey, 1990; Cervetto & Piccolino, 1974; Thoreson, 1999). By contrast, prolonged hypoxia resulted in a clear reduction in glutamate responses. Median peak current density declined by ~10.5% after 15 min of hypoxic exposure. This effect was absent in an identical protocol conducted under normoxia, where responses remained stable across all three glutamate applications. The stability of recordings during normoxia indicate that receptor desensitization or cell rundown did not contribute to the observed iGluR suppression, suggesting that hypoxia alone induced the reduction in receptor activity at the plasma membrane.

4.2 Sustained Suppression After Reoxygenation

HCs were subjected to three sequential applications of glutamate, each delivered at a distinct time point to determine if the suppressed response was reversible upon reoxygenation. After 15 min of hypoxia, mean peak current density decreased by ~16%. This confirms previous results that continuous hypoxic exposure was sufficient to induce iGluR suppression. However, current density following reoxygenation did not significantly recover. The absence of a significant recovery within this timeframe suggests that 10 min of restored P_{O2} could be insufficient to reverse the effects of hypoxia on glutamate receptor currents. However, this lack of recovery should not be interpreted as evidence of irreversibility. Rather, it is likely that the recovery process requires a longer reoxygenation period. Indeed, in other hypoxia-tolerant vertebrate systems, recovery from hypoxic suppression often requires a reoxygenation period longer than 10 min. In crucian carp, supressed responses in the retina required approximately 45 min of normoxia to recover from a 90% suppression (Johansson et al., 1997). Similarly, in hippocampal slices of the naked mole rat, synaptic activity remained supressed after 30 min of anoxia and recovered after 30-60 min reoxygenation periods (Larson & Park, 2009). Additional studies have shown that recovery of neural responses to baseline excitability following anoxia can require prolonged periods of restored oxygen availability, likely due to the time needed to reestablish ionic gradients and recover from metabolic stress (Money et al., 2014; Edelman et al., 1991). It is therefore possible that goldfish HCs require reoxygenation periods longer than 10 min as well to fully recover from the hypoxia-induced suppression of glutamate receptors. Due to technical limitations in maintaining stable patch-clamp recordings for extended durations, we were unable to assess recovery beyond 10 min. Future work extending reoxygenation periods could provide further insight into the reversibility of this adaptive response.

4.3 mK_{ATP} Channel Activation as a Sensor and Mediator of Receptor Downregulation

In the current study, the decrease in iGluR activity during hypoxia depended on the activation of mK_{ATP} channels, as blocking these channels with glibenclamide eliminated the suppressed response. In earlier work from our lab, fluorescence of tetramethylrhodamine ethyl ester (TMRE) dye was used to monitor changes in $\Delta\psi m$ from goldfish HCs. TMRE fluorescence increased significantly within the first 5 min of hypoxia, but this response was reduced in the presence of mK_{ATP} antagonists, like 5-hydroxydecanoate (5-HD) and glibenclamide. These findings indicated that mK_{ATP} channels are activated during the first few minutes of hypoxia and could be functioning as metabolic sensors (Country & Jonz, 2021) that activate during low oxygen periods to trigger a neuroprotective response. In several animal models, activation of mK_{ATP} channels during hypoxia serves as the initiating signal for neuroprotection. In the mammalian retina, brief ischemic or hypoxic preconditioning has been shown to protect neurons against subsequent injury, with the opening of mK_{ATP} channels playing a central role in this response (Yamauchi et al., 2003; Roth, 2004; Roth et al., 2006). Similarly, in primary rat cortical neurons, opening of these mK_{ATP} channels preconditioned cells against glutamate excitotoxicity and oxygen deprivation (Kis et al., 2004). In the anoxia-tolerant turtle, mK_{ATP} activation suppressed AMPAR currents by 52% during anoxia and activation of mK_{ATP} channels during normoxia produced a similar decrease in AMPAR activity (Zivkovic & Buck, 2010). In the hypoxia-intolerant rainbow trout, activation of these channels with diazoxide maintained $[Ca^{2+}]_i$ during hypoxia, whereas without activation, $[Ca^{2+}]_i$ rose to excitotoxic levels within 20 min (Country & Jonz, 2021). When mK_{ATP} channels open during anoxia, the mitochondrial membrane potential slightly depolarizes due to the partial dissipation of the mitochondrial H^+ gradient. This results in a modest increase in cytosolic Ca^{2+} due to a reduction in the driving

force of the MCU, which limits Ca^{2+} uptake into the mitochondria, as well as increases Ca^{2+} release from the mitochondrial membrane transition pore (MPTP) (Pamenter, 2014; Buck & Pamenter, 2018; Hawrysh & Buck, 2013). In HCs, CICR also plays an important role in regulating Ca^{2+} dynamics (reviewed in Country & Jonz, 2017). Calcium imaging experiments in the carp retina have shown that, in the presence of glutamate, there is a large transient peak in $[Ca^{2+}]_i$ that is blocked by ryanodine, suggesting it is released from CICR through ER stores (reviewed in Country & Jonz, 2017; Huang et al., 2004). Thus, it was important to determine whether cytosolic Ca^{2+} was mediating the suppressed response during hypoxia.

4.4 A Potential Role for Intracellular Ca^{2+} in Hypoxia Tolerance

As predicted, blocking Ca^{2+} uptake via the MCU prevented the suppression of iGluR currents under hypoxia, suggesting that mitochondrial cytosolic Ca^{2+} buffering contributes to this response. When the MCU was inhibited with 400 nM ruthenium red, glutamate responses remained stable throughout hypoxia, with no significant difference between the first and third bouts. Similarly, in preliminary experiments blocking Ca^{2+} release from the ER with 20 μM ryanodine produced the same outcome. Although inhibition of the MCU would reduce mitochondrial Ca^{2+} buffering and potentially increase cytosolic Ca^{2+}, uptake through the MCU under hypoxia may potentially serve to maintain $[Ca^{2+}]_i$ at levels that evade excitotoxicity (Nicholls & Budd, 2000; Rizzuto et al., 2012) while also contributing to the regulated Ca^{2+} signal. These findings support those of Nagy-Watson & Jonz who found that blocking the MCU or ryanodine receptors in the ER abolished a hypoxia-induced rise in intracellular Ca^{2+} in goldfish HCs, supporting the idea that both the mitochondria and ER contribute to initiating the neuroprotective suppression of iGluR activity (2025). In further support of this Ca^{2+} dependent

mechanism, chelation of intracellular Ca^{2+} with 50 μM of BAPTA-AM abolished the hypoxic response as shown in the single cell recording obtained, with glutamate currents remaining stable across all bouts. While this observation is based on a limited sample size, it is consistent with the effects of inhibiting the MCU and ryanodine receptors and suggests that Ca^{2+} release into the cytosol contributes to mediating these changes in the membrane. However, these experiments were not pursued further because incubating cells in BAPTA-AM impaired seal formation, reducing the number of successful patch-clamp experiments.

In the present model, we propose that during the early stages of hypoxia in the retina, mK_{ATP} channels are activated allowing HCs to maintain $[Ca^{2+}]_i$ (Country & Jonz, 2021). Paradoxically, Ca^{2+} is released from internal stores resulting in a modest yet significant rise in $[Ca^{2+}]_i$ (Nagy-Watson & Jonz, 2025). This controlled rise in $[Ca^{2+}]_i$ then engages downstream pathways that suppress iGluR activity at the membrane. The proposed pathway is similar to a mechanism described in the cortex of the anoxia-tolerant turtle brain (Pamenter & Buck, 2008). The modest rise in cytosolic Ca^{2+} acts as a signalling cue that interacts with calmodulin which in turn inhibits NMDARs and promotes channel arrest (Pamenter et al., 2008; reviewed in Buck & Pamenter, 2018; Shin et al., 2005; Ehlers et al., 1996; Krupp et al., 1999; Chowdhury et al., 2017). Complementary work in the same species demonstrated that AMPARs are also downregulated during anoxia (Pamenter et al., 2007). Together, these findings suggest that a similar pathway may occur in goldfish HCs, where AMPAR suppression could be the primary mechanism for the observed decrease in glutamate-activated currents, ultimately conserving energy and reducing Ca^{2+} influx during hypoxia. This is especially likely given that Ca^{2+} permeable AMPARs are the most prominent iGluR type in *Carassius* HCs (Sun et al., 2010). This mechanism is summarized in Figure 9. This model is supported by the work of Johansson et

al. (1997), who demonstrated that retinal responses are strongly suppressed during anoxia in crucian carp. In this context, the suppression of iGluR activity in HCs would decrease excitability in HCs, potentially contributing to overall reduction in retinal activity. The presented mechanism may also promote glutamate release from photoreceptors. Suppression of iGluR activity would hyperpolarize HCs, which would reduce proton-mediated inhibition of presynaptic Ca^{2+} channels. The resulting increase in Ca^{2+} influx would increase glutamate release from photoreceptors, which in turn would hyperpolarize ON bipolar cells. Whether this response depends solely on HCs as hypoxia sensors or also involves other retinal neurons remains to be determined.

4.5 Ionotropic Glutamate Receptor Suppression in Hypoxia May Occur Independently of GABA Signaling

To assess whether the rise in $[Ca^{2+}]_i$ might be involved in the GABA release mechanism from HCs, we used mass spectrometry to quantify $[GABA]_e$ under different treatment conditions. Across treatment groups, the data ultimately lacked a consistent trend in $[GABA]_e$, suggesting that hypoxia did not increase GABA release. These results argue against the idea that Ca^{2+} in HCs could be acting primarily to increase GABA release onto photoreceptors during hypoxia to supress retinal activity. Instead, the absence of a clear increase in $[GABA]_e$, combined with the evidence that blocking Ca^{2+} from internal stores abolishes iGluR suppression, supports the interpretation that the modest Ca^{2+} rise reported in Nagy-Watson & Jonz (2025) serves mainly to suppress glutamate receptor activity.

Figure 9. Working model of a hypoxia tolerance mechanism through which intracellular Ca^{2+} signalling induces the downregulation of ionotropic glutamate receptors in horizontal cells of goldfish retina. Starting at the upper left, hypoxia ($\downarrow PO_2$) leads to a decline in ATP levels in both photoreceptors and HCs, as reduced oxygen availability limits ATP production through oxidative phosphorylation (1). In photoreceptors, this decrease in ATP availability leads to uncontrolled depolarization and excessive glutamate release, which activates ionotropic glutamate receptors (iGluR, purple) on the HC membrane. Binding of glutamate increases inward Na^+ current, resulting in the depolarization of the membrane (ΔVm) and subsequent opening of voltage gated Ca^{2+} channels (VGCC, blue) (2). In HCs, hypoxia also reduces ATP production which lowers the ATP:ADP ratio and thereby triggers the opening of mitochondrial ATP-dependent K^+ channels (mK_{ATP}, green) on the inner mitochondrial membrane (Tinker et al., 2013) (3). The activation of these channels increases K^+ influx in the mitochondrion which leads to ion exchange (K^+/H^+ exchanger, red) and produces a modest depolarization of the mitochondrial membrane potential ($\Delta\psi$m). This reduces the uptake of Ca^{2+} via the mitochondrial Ca^{2+} uniporter (MCU, grey), allowing cytosolic Ca^{2+} levels to rise (4). Together with Ca^{2+} entry through VGCCs in the membrane, this signal promotes Ca^{2+}-induced Ca^{2+} release from endoplasmic reticulum (ER) via ryanodine receptors (RyR, yellow) (5), which ultimately further increases $[Ca^{2+}]_i$ (6). Elevated $[Ca^{2+}]_i$ activates calmodulin (CalM), which may interact with iGluRs at the plasma membrane to reduce their activity (7). This model is supported by evidence from goldfish HCs (Country & Jonz, 2021; Nagy-Watson & Jonz, 2025; reviewed in Jonz, 2025) as well as a similar mechanism described in the anoxia-tolerant turtle brain (Buck & Pamenter, 2018; Pamenter et al., 2008). Through this mechanism, mK_{ATP} activation and subsequent Ca^{2+} signalling work together to reduce excitotoxic glutamatergic responses during hypoxia by

conserving energy and limiting Ca^{2+} overload. For further details, see text. Created using BioRender.com

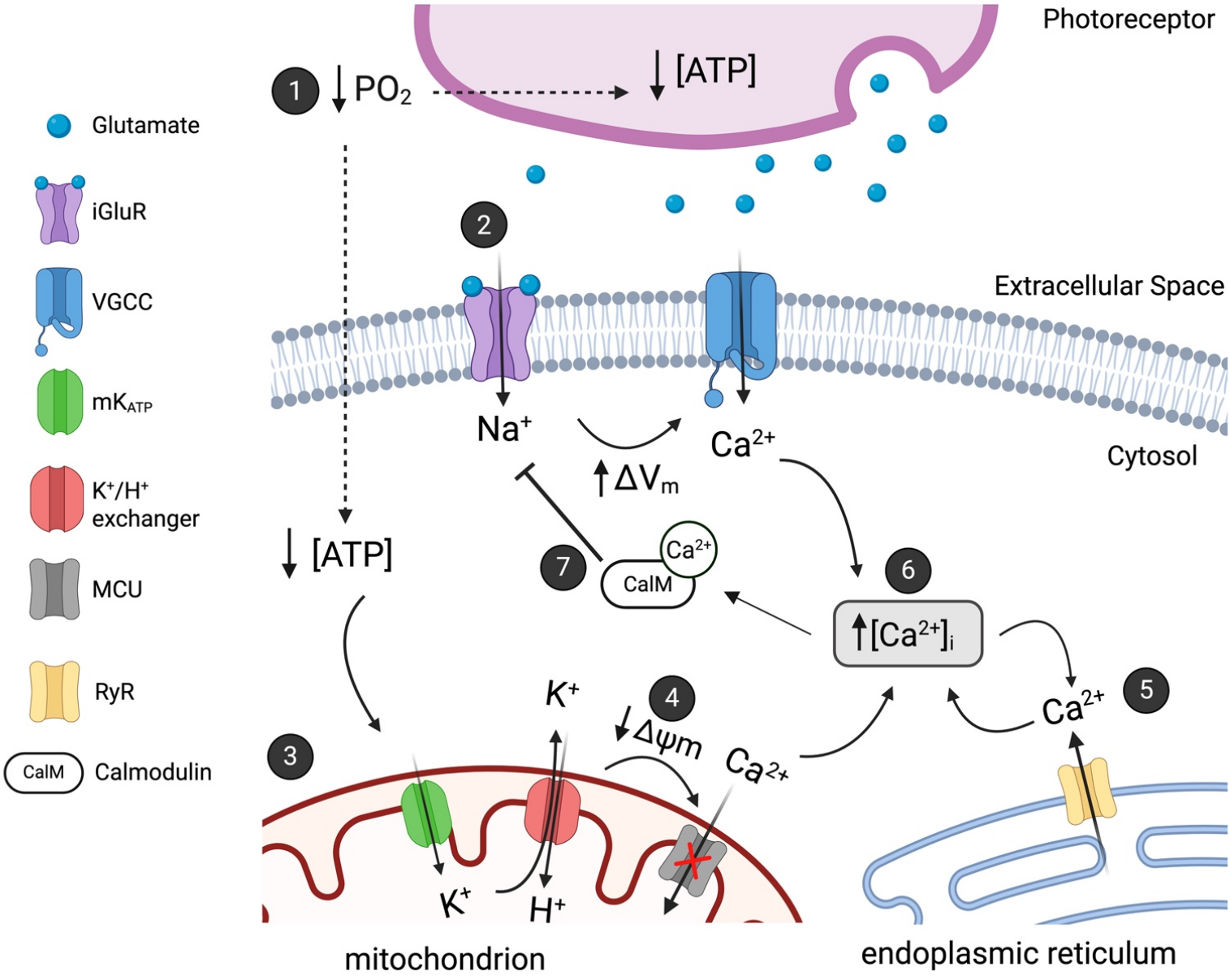
Photoreceptor
1
PO_2
[ATP]
Glutamate
iGluR
VGCC
mK_{ATP}
K^+/H^+ exchanger
MCU
RyR
CalM
Calmodulin
2
Extracellular Space
Na^+
Ca^{2+}
$\uparrow\Delta V_m$
Cytosol
[ATP]
7
Ca^{2+}
CalM
6
$\uparrow[Ca^{2+}]_i$
K^+
4
$\downarrow\Delta\psi m$
Ca^{2+}
Ca^{2+}
5
3
K^+
H^+
mitochondrion
endoplasmic reticulum

Figure 9

5. CONCLUSION

The present study demonstrates that iGluR activity in goldfish HCs is significantly reduced during hypoxia, and that this suppression is dependent on the activation of mK_{ATP} channels. Activation of these channels initiates a controlled rise in intracellular Ca^{2+} from internal stores (Nagy-Watson & Jonz, 2025), which may serve as a signal to downregulate glutamate receptor activity while also preventing excitotoxic Ca^{2+} accumulation (Country & Jonz, 2021). A similar Ca^{2+} dependent suppression pathway has been described in the anoxia-tolerant turtle cortex (Pamenter et al., 2008), suggesting a conserved neuroprotective strategy among vertebrates under metabolic stress. These findings provide insight into a potential mechanism in goldfish retina, where receptor activity in the membrane is modulated to reduce metabolic demand, maintain $[Ca^{2+}]_i$ and preserve cell viability during stress. Taken together, these results suggest that HCs act as sensors of hypoxia in goldfish, initiating a response that maintains retinal function. Whether other retinal neurons also exhibit a similar sensitivity to oxygen availability remains an open question. Future studies should clarify the downstream signalling pathways and identify the specific receptor subtypes involved in this suppression to better understand both how goldfish HCs tolerate hypoxia and how hypoxia tolerance is coordinated across neurons in the retina.

REFERENCES

Ames III, A. (1992). Energy requirements of CNS cells as related to their function and to their vulnerability to ischemia: A commentary based on studies on Retina. *Canadian Journal of Physiology and Pharmacology*, *70*(S1). https://doi.org/10.1139/y92-257

Ayoub, G.S. & Lam, D.M. (1985). The content and release of endogenous GABA in isolated 474 horizontal cells of the goldfish retina. Vision Res 25, 1187-1193.

Ayoub, G. S., & Lam, D. M. (1984). The release of gamma-aminobutyric acid from horizontal cells of the goldfish (carassius auratus) retina. The Journal of Physiology, 355(1), 191–214. https://doi.org/10.1113/jphysiol.1984.sp015414f

Barnes, S., Grove, J. C., McHugh, C. F., Hirano, A. A., & Brecha, N. C. (2020). Horizontal cell feedback to cone photoreceptors in mammalian retina: Novel insights from the GABA-ph hybrid model. Frontiers in Cellular Neuroscience, 14. https://doi.org/10.3389/fncel.2020.595064

Buck, L. T., & Pamenter, M. E. (2018). The hypoxia-tolerant vertebrate brain: Arresting synaptic activity. Comparative Biochemistry and Physiology Part B: Biochemistry and Molecular Biology, 224, 61–70. https://doi.org/10.1016/j.cbpb.2017.11.015

Byzov, A. L., & Shura-Bura, T. M. (1986). Electrical feedback mechanism in the processing of signals in the outer plexiform layer of the retina. *Vision Research*, *26*(1), 33–44.

Cervetto, L., & Piccolino, M. (1974). Synaptic transmission between photoreceptors and horizontal cells in the turtle retina. *Science*, *183*(4123), 417–419. https://doi.org/10.1126/science.183.4123.417

Choi, D. W. (1992). Excitotoxic Cell death. Journal of Neurobiology, 23(9), 1261–1276. https://doi.org/10.1002/neu.480230915

Chowdhury, D., Turner, M., Patriarchi, T., Hergarden, A. C., Anderson, D., Zhang, Y., Sun, J., Chen, C., Ames, J. B., & Hell, J. W. (2017). Ca2+/calmodulin binding to psd-95 mediates homeostatic synaptic scaling down. *The EMBO Journal*, *37*(1), 122–138. https://doi.org/10.15252/embj.201695829

Country, M. W., & Jonz, M. G. (2021). Mitochondrial KATP channels stabilize intracellular ca2+ during hypoxia in retinal horizontal cells of goldfish (*carassius auratus*). *Journal of Experimental Biology*, *224*(18). https://doi.org/10.1242/jeb.242634

Country, M. W., & Jonz, M. G. (2022). Goldfish and Crucian Carp are natural models of anoxia tolerance in the retina. Comparative Biochemistry and Physiology Part A: Molecular & Integrative Physiology, 270, 111244. https://doi.org/10.1016/j.cbpa.2022.111244

Country, M. W. (2017). Retinal metabolism: A comparative look at energetics in the Retina. *Brain Research*, *1672*, 50–57. https://doi.org/10.1016/j.brainres.2017.07.025

Diamond, J. S. (2011). Calcium-permeable AMPA receptors in the retina. Frontiers in Molecular Neuroscience, 4. https://doi.org/10.3389/fnmol.2011.00027

Dingledine, R., Borges, K., Bowie, D., & Traynelis, S. F. (1999). The glutamate receptor ion channels. Pharmacological Reviews, 51(1), 7–61. https://doi.org/10.1016/s0031-6997(24)01394-2

Dowling, J. E., & Ripps, H. (1973). Effect of Magnesium on Horizontal Cell Activity in the Skate Retina. Nature, 242(5393), 101–103. https://doi.org/10.1038/242101a0

Dowling, J. E. (1987). *The Retina*. https://doi.org/10.2307/j.ctv31zqj2d

Edelman, N. H., Melton, J. E., & Neubauer, J. A. (1991). Central adaptation to hypoxia. *Response and Adaptation to Hypoxia*, 235–244. https://doi.org/10.1007/978-1-4614-7574-3_22

Ehlers, M. D., Zhang, S., Bernhardt, J. P., & Huganir, R. L. (1996). Inactivation of NMDA receptors by direct interaction of calmodulin with the NR1 subunit. *Cell*, *84*(5), 745–755. https://doi.org/10.1016/s0092-8674(00)81052-1

Grigoryan, E. N. (2022). Self-organization of the retina during eye development, retinal regeneration in vivo, and in retinal 3D organoids in vitro. Biomedicines, 10(6), 1458. https://doi.org/10.3390/biomedicines10061458

Hawrysh, P.J., and Buck, L.T. (2013). Anoxia-mediated calcium release through the mitochondrial permeability transition pore silences NMDA receptor cur- rents in turtle neurons. J. Exp. Biol. 216(23): 4375–4387. doi:10.1242/jeb. 092650. PMID:24259257.

Hirano, A. A., Liu, X., Boulter, J., Grove, J., Pérez de Sevilla Müller, L., Barnes, S., & Brecha, N. C. (2016). Targeted Deletion of Vesicular GABA Transporter from Retinal Horizontal Cells Eliminates Feedback Modulation of Photoreceptor Calcium Channels. Eneuro, 3(1), ENEURO.0148-15.2016.

Hoon M, Okawa H, Della Santina L, Wong RO. (2014). Functional architecture of the retina: development and disease. Prog Retin Eye Res. 2014 Sep;42:44-84. doi: 10.1016/j.preteyeres.2014.06.003. Epub 2014 Jun 28. PMID: 24984227; PMCID: PMC4134977

Huang SY, Liu Y, Liang PJ. (2004). Role of Ca2+ store in AMPA-triggered Ca2 dynamics in retinal horizontal cells. Neuroreport 15: 2311–2315.

Jacoby, J., Kreitzer, M. A., Alford, S., Qian, H., Tchernookova, B. K., Naylor, E. R., & Malchow, R. P. (2012). Extracellular pH dynamics of retinal horizontal cells examined using electrochemical and fluorometric methods. Journal of Neurophysiology, 107(3), 868–879.

Johansson, D., Nilsson, G. E., & Törnblom, E. (1995). Effects of anoxia on energy metabolism in crucian carp brain slices studied with microcalorimetry. Journal of Experimental Biology, 198(3), 853–859. https://doi.org/10.1242/jeb.198.3.853

Johansson, D., Nilsson, G. E., & Døving, K. B. (1997). Anoxic depression of light-evoked potentials in retina and optic tectum of crucian carp. Neuroscience Letters, 237(2–3), 73–76. https://doi.org/10.1016/s0304-3940(97)00814-8

Jonz, M. G. (2025). Adaptations to hypoxia in the vertebrate retina. *The Journal of Physiology*. https://doi.org/10.1113/jp287741

Jonz, M. G., & Barnes, S. (2007). Proton modulation of ion channels in isolated horizontal cells of the goldfish retina. The Journal of Physiology, 581(2), 529–541.

Jonz, M. G., Fearon, I. M., & Nurse, C. A. (2004). Neuroepithelial oxygen chemoreceptors of the zebrafish gill. The Journal of Physiology, 560(3), 737–752. https://doi.org/10.1113/jphysiol.2004.069294

Kis, B., Nagy, K., Snipes, J. A., Rajapakse, N. C., Horiguchi, T., Grover, G. J., & Busija, D. W. (2004). The mitochondrial KATP channel opener BMS-191095 induces neuronal preconditioning. NeuroReport, 15(2), 345–349. https://doi.org/10.1097/00001756-200402090-00027

Kolb H. Simple Anatomy of the Retina. (1995). In: Webvision: The Organization of the Retina and Visual System. University of Utah Health Sciences Center, Salt Lake City (UT).

Krupp, J. J., Vissel, B., Thomas, C. G., Heinemann, S. F., & Westbrook, G. L. (1999). Interactions of calmodulin and α-actinin with the NR1 subunit modulate ca2+-dependent inactivation of NMDA receptors. *The Journal of Neuroscience*, *19*(4), 1165–1178. https://doi.org/10.1523/jneurosci.19-04-01165.1999

Lam, D. M., Lasater, E. M., & Naka, K. I. (1978). Gamma-aminobutyric acid: A neurotransmitter candidate for cone horizontal cells of the catfish retina. Proceedings of the National Academy of Sciences, 75(12), 6310–6313. https://doi.org/10.1073/pnas.75.12.6310

Larson, J., & Park, T. J. (2009). Extreme hypoxia tolerance of naked mole-rat brain. *NeuroReport*, *20*(18), 1634–1637. https://doi.org/10.1097/wnr.0b013e32833370cf

Linn, C., & Christensen, B. (1992). Excitatory amino acid regulation of intracellular Ca2+ in isolated catfish cone horizontal cells measured under voltage- and concentration- clamp conditions. The Journal of Neuroscience, 12(6), 2156–2164.

Liu, S.-Q. J., & Cull-Candy, S. G. (2000). Synaptic activity at calcium-permeable AMPA receptors induces a switch in receptor subtype. Nature, 405(6785), 454–458. https://doi.org/10.1038/35013064

Liu, D., Lu, C., Wan, R., Auyeung, W. W., & Mattson, M. P. (2002). Activation of mitochondrial ATP-dependent potassium channels protects neurons against ischemia-induced death by a mechanism involving suppression of BAX translocation and cytochrome c release. Journal of Cerebral Blood Flow & Metabolism, 22(4), 431–443. https://doi.org/10.1097/00004647-200204000-00007

Marc, R. E., Stell, W. K., Bok, D., & Lam, D. M. (1978). GABA-ergic pathways in the Goldfish Retina. Journal of Comparative Neurology, 182(2), 221–245. https://doi.org/10.1002/cne.901820204

Masland, R. H. (2012). The neuronal organization of the Retina. *Neuron*, *76*(2), 266–280. https://doi.org/10.1016/j.neuron.2012.10.002

Massey, S. C. (1990). Chapter 11 cell types using glutamate as a neurotransmitter in the vertebrate retina. Progress in Retinal Research, 9, 399–425. https://doi.org/10.1016/0278-4327(90)90013-8

Mayer, M. L., Westbrook, G. L., & Guthrie, P. B. (1984). Voltage-dependent block by mg2+ of NMDA responses in spinal cord neurones. Nature, 309(5965), 261–263. https://doi.org/10.1038/309261a0

Miller, A. M., & Schwartz, E. A. (1983). Evidence for the identification of synaptic transmitters released by photoreceptors of the toad retina. The Journal of Physiology, 334(1), 325–349.

Money, T. G., Sproule, M. K., Hamour, A. F., & Robertson, R. M. (2014). Reduction in neural performance following recovery from anoxic stress is mimicked by AMPK pathway activation. *PLoS ONE*, *9*(2). https://doi.org/10.1371/journal.pone.0088570

Neves, G., & Lagnado, L. (1999). The Retina. *Current Biology*, *9*(18). https://doi.org/10.1016/s0960-9822(99)80436-9

Nicholls, D. G., & Budd, S. L. (2000). Mitochondria and neuronal survival. Physiological Reviews, 80(1), 315–360. https://doi.org/10.1152/physrev.2000.80.1.315

Nilsson, Göran E. (1992). Evidence for a role of GABA in metabolic depression during anoxia in crucian carp (carassius carassius). Journal of Experimental Biology, 164(1), 243–259. https://doi.org/10.1242/jeb.164.1.243

Nilsson, G. E., & Lutz, P. L. (1991). Release of inhibitory neurotransmitters in response to anoxia in Turtle Brain. American Journal of Physiology-Regulatory, Integrative and Comparative Physiology, 261(1). https://doi.org/10.1152/ajpregu.1991.261.1.r32

Nilsson, G. E. and Lutz, P. L. (2004). Anoxia tolerant brains. J. Cereb. Blood Flow Metab. 24, 475-486. doi:10.1097/00004647-200405000-00001

Nagy-Watson, N. V., & Jonz, M. G. (2025). Hypoxia increases intracellular calcium in glutamate-activated horizontal cells of goldfish retina via mitochondrial KATP channels and intracellular stores. *Comparative Biochemistry and Physiology Part A: Molecular & Integrative Physiology*, *300*, 111786. https://doi.org/10.1016/j.cbpa.2024.111786

Orrenius, S., & Nicotera, P. (1994). The calcium ion and cell death. Journal of Neural Transmission. Supplementum, 43, 1–11.

Orrenius, S., Zhivotovsky, B., & Nicotera, P. (2003). Regulation of cell death: the calcium–apoptosis link. Nature Reviews Molecular Cell Biology, 4(7), 552–565

Pamenter, M. E., Shin, D. S.-H., & Buck, L. T. (2007). AMPA receptors undergo channel arrest in the anoxic turtle cortex. American Journal of Physiology-Regulatory, Integrative and Comparative Physiology, 294(2). https://doi.org/10.1152/ajpregu.00433.2007

Pamenter, M. E., Shin, D. S., Cooray, M., & Buck, L. T. (2008). Mitochondrial ATP-sensitive K+ channels regulate NMDAR activity in the cortex of the anoxic western painted turtle. *The Journal of Physiology*, *586*(4), 1043–1058. https://doi.org/10.1113/jphysiol.2007.142380

Pamenter, Matthew E., Hogg, D. W., Ormond, J., Shin, D. S., Woodin, M. A., & Buck, L. T. (2011). Endogenous GABAa and GABAb receptor-mediated electrical suppression is critical to neuronal anoxia tolerance. Proceedings of the National Academy of Sciences, 108(27), 11274–11279. https://doi.org/10.1073/pnas.1102429108

Pamenter Matthew E.. 2014. Mitochondria: a multimodal hub of hypoxia tolerance. Canadian Journal of Zoology. 92(7): 569-589. https://doi.org/10.1139/cjz-2013-0247

Paoletti, P., Bellone, C., & Zhou, Q. (2013). NMDA receptor subunit diversity: Impact on receptor properties, synaptic plasticity and disease. Nature Reviews Neuroscience, 14(6), 383–400. https://doi.org/10.1038/nrn3504

Peng PL, Zhong X, Tu W, Soundarapandian MM, Molner P, Zhu D, Lau L, Liu S, Liu F, Lu Y. ADAR2-dependent RNA editing of AMPA receptor subunit GluR2 determines vulnerability of neurons in forebrain ischemia. Neuron 49: 719–733, 2006.

Quinn, N., Csincsik, L., Flynn, E., Curcio, C. A., Kiss, S., Sadda, S. R., Hogg, R., Peto, T., & Lengyel, I. (2019). The clinical relevance of visualising the peripheral retina. Progress in Retinal and Eye Research, 68, 83–109. https://doi.org/10.1016/j.preteyeres.2018.10.001

Rizzuto, R., De Stefani, D., Raffaello, A., & Mammucari, C. (2012). Mitochondria as sensors and regulators of calcium signalling. Nature Reviews Molecular Cell Biology, 13(9), 566–578. https://doi.org/10.1038/nrm3412

Rosales, C. A., Lepinsky, N. A., Ramadan, M., Manthorpe, J. M., Jonz, M. G., & Smith, J. C. (2025). Enhanced LC-MS detection of γ-aminobutyric acid via trimethylation enhancement using diazomethane. *Journal of the American Society for Mass Spectrometry*, *36*(12), 2699–2706. https://doi.org/10.1021/jasms.5c00294

Roth, S., Dreixler, J. C., Shaikh, A. R., Lee, K. H., & Bindokas, V. (2006a). Mitochondrial potassium ATP channels and retinal ischemic preconditioning. *Investigative Opthalmology & Visual Science*, *47*(5), 2114. https://doi.org/10.1167/iovs.05-1068

Roth, S. (2004). Endogenous neuroprotection in the retina. *Brain Research Bulletin*, *62*(6), 461–466. https://doi.org/10.1016/j.brainresbull.2003.07.006

Shin, D. S.-H., Wilkie, M. P., Pamenter, M. E., & Buck, L. T. (2005). Calcium and protein phosphatase 1/2A attenuate N-methyl-D-aspartate receptor activity in the anoxic turtle cortex. Comparative Biochemistry and Physiology Part A: Molecular & Integrative Physiology, 142(1), 50–57. https://doi.org/10.1016/j.cbpa.2005.07.017

Stell, W. K., & Lightfoot, D. O. (1975). Color-specific interconnections of cones and horizontal cells in the retina of the Goldfish. Journal of Comparative Neurology, 159(4), 473–501. https://doi.org/10.1002/cne.901590404

Sun, Y., Jiang, X.-D., Liu, X., Gong, H.-Q., & Liang, P.-J. (2010). Synaptic contribution of ca2+-permeable and ca2+-impermeable AMPA receptors on isolated carp retinal horizontal cells and their modulation by zn2+. *Brain Research*, *1317*, 60–68. https://doi.org/10.1016/j.brainres.2009.12.068

Szydlowska, K., & Tymianski, M. (2010). Calcium, ischemia and excitotoxicity. Cell Calcium, 47(2), 122–129.

Tachibana M. (1983). Ionic currents of solitary horizontal cells isolated from goldfish retina. The Journal of physiology, 345, 329–351.

Thoreson, W. (1999). Glutamate receptors and circuits in the vertebrate retina. *Progress in Retinal and Eye Research*, *18*(6), 765–810. https://doi.org/10.1016/s1350-9462(98)00031-7

Thoreson, W. B., & Mangel, S. C. (2012). Lateral interactions in the outer retina. Progress in Retinal and Eye Research, 31(5), 407–441. https://doi.org/10.1016/j.preteyeres.2012.04.003

Tinker, A., Aziz, Q., & Thomas, A. (2013a). The role of atp-sensitive potassium channels in cellular function and protection in the cardiovascular system. *British Journal of Pharmacology*, *171*(1), 12–23. https://doi.org/10.1111/bph.12407

Verweij, J., Kamermans, M., & Spekreijse, H. (1996). Horizontal cells feed back to cones by shifting the cone calcium-current activation range. Vision Research, 36(24), 3943–3953. https://doi.org/10.1016/s0042-6989(96)00142-3

Verkhratsky, A. (2007). Calcium and Cell Death. In: Carafoli, E., Brini, M. (eds) Calcium Signalling and Disease. Subcellular Biochemistry, vol 45. Springer, Dordrecht. https://doi.org/10.1007/978-1-4020-6191-2_1

Vroman, R., Klaassen, L. J., & Kamermans, M. (2013). Ephaptic communication in the vertebrate retina. Frontiers in Human Neuroscience, 7.

Walker, R. M. and Johansen, P. H. (1977). Anaerobic metabolism in goldfish (Carassius auratus). Can. J. Zool. 55, 1304-1311. doi:10.1139/z77-170

Wei, J., & Yang, X. (1997). Effects of acute hypoxia on responses of rod- and cone-driven horizontal cells in carp retinain vivo. Chinese Science Bulletin, 42(4), 341–344. https://doi.org/10.1007/bf02882478

Wilkie, M. P., Pamenter, M. E., Alkabie, S., Carapic, D., Shin, D. S. H., & Buck, L. T. (2008). Evidence of anoxia-induced channel arrest in the brain of the goldfish (carassius auratus). Comparative Biochemistry and Physiology Part C: Toxicology & Pharmacology, 148(4), 355–362. https://doi.org/10.1016/j.cbpc.2008.06.004

Wind, T., Prehn, J. H. M., Peruche, B., & Krieglstein, J. (1997). Activation of ATP-sensitive potassium channels decreases neuronal injury caused by chemical hypoxia. Brain Research, 751(2), 295–299. https://doi.org/10.1016/s0006-8993(96)01419-9

Wright, A., & Vissel, B. (2012). The essential role of AMPA receptor GluR2 subunit RNA editing in the normal and diseased brain. Frontiers in Molecular Neuroscience, 5.

Wong-Riley, M. (2010). Energy metabolism of the visual system. *Eye and Brain*, 99. https://doi.org/10.2147/eb.s9078

Yamauchi, T., Kashii, S., Yasuyoshi, H., Zhang, S., Honda, Y., & Akaike, A. (2003). Mitochondrial ATP-sensitive potassium channel: A novel site for neuroprotection. *Investigative Opthalmology & Visual Science*, *44*(6), 2750. https://doi.org/10.1167/iovs.02-0815

Zivkovic, G., & Buck, L. T. (2010). Regulation of AMPA receptor currents by mitochondrial ATP-sensitive K+channels in anoxic turtle neurons. Journal of Neurophysiology, 104(4), 1913–1922. https://doi.org/10.1152/jn.00506.2010

6. APPENDIX

6.1 Preliminary Experiments

Figure A1. Inhibition of intracellular Ca^{2+} release from ryanodine receptors abolished suppression of iGluR currents during hypoxia. (**A**) Representative recording from a cell treated with a co-application of 20 μM ryanodine with 100 μM glutamate under continuous hypoxia. (**B**) Summary data of HCs treated with ryanodine ($N = 2$ from 2 fish) showing no significance between the first and third bouts. Blockage of the MCU (with ruthenium red) or ryanodine receptors in the ER (with ryanodine) prevented the reduction in iGluR activity in hypoxia. Each point represents an individual cell. Data are presented as medians with interquartile range.

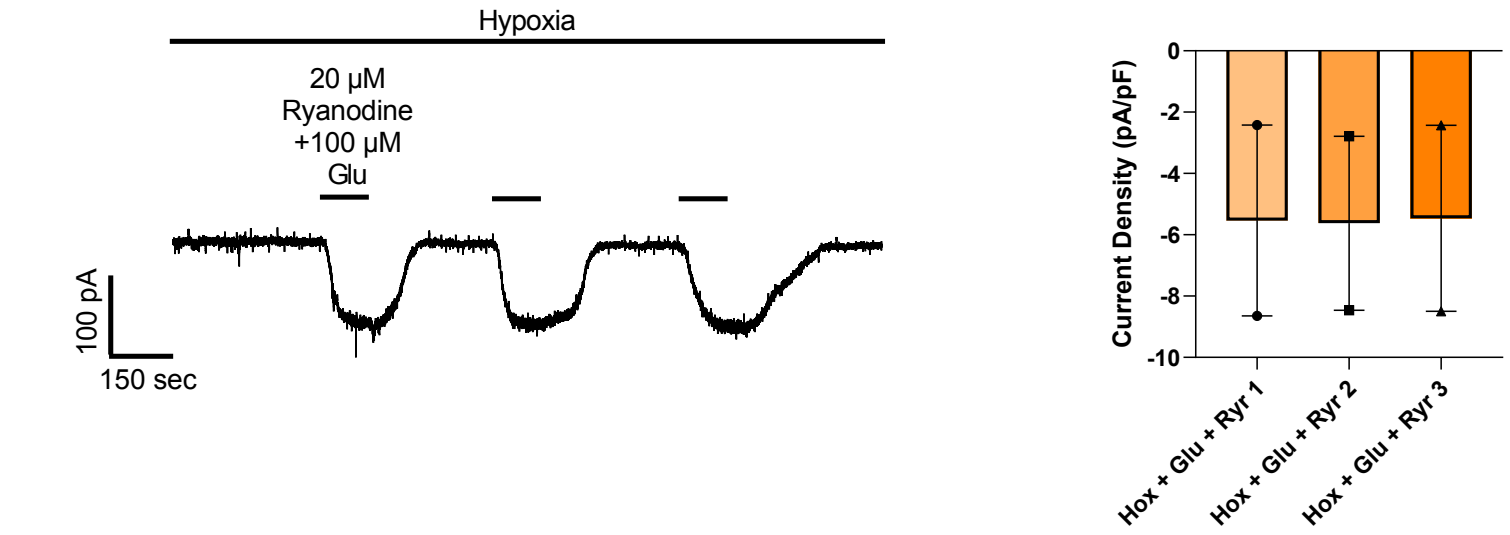
A
Hypoxia
20 μM
Ryanodine
+100 μM
Glu
100 pA
150 sec
B
Current Density (pA/pF)
0
-2
-4
-6
-8
-10
Hox + Glu + Ryr 1
Hox + Glu + Ryr 2
Hox + Glu + Ryr 3

Figure A1

Figure A2. Chelation of intracellular calcium prevented hypoxic suppression of iGluR currents. Gap free recording clamped at -60 mV where glutamate was applied under continuous hypoxia for 2 min at 5 min intervals throughout the recording. HCs were incubated with 50 μM BAPTA-AM followed by a 10 min wash in ECS. The representative trace shows stable glutamate activated current amplitudes across all applications, indicating that buffering out intracellular calcium abolished the hypoxia induced decrease in iGluR activity.

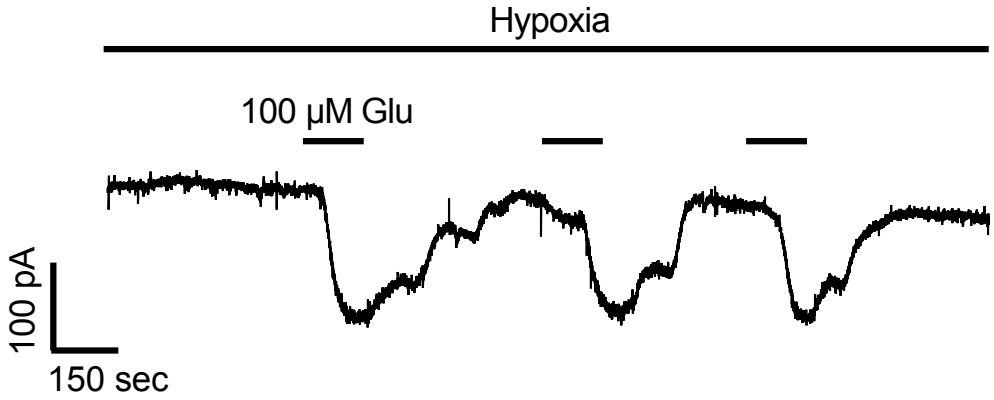

Figure A2